Lignin acrylic acid polymer as an emulsifier for oil-water emulsions

By

Shirin Fatehi

Supervisors:

Dr. Leila Pakzad

Dr. Ehsan Behzadfar

A thesis submitted in the partial

fulfillment of the requirements for the degree of Master of Science

Environmental Engineering Program

Dedication

To my parents for their unconditional support

Abstract

Oil-water emulsions are applied in various fields such as food, cosmetics, pharmaceuticals, petro-chemicals, and agricultural products. Currently, synthetic-based emulsifiers are extensively used in oil-water emulsions, but the use of synthetic emulsifiers is discouraged due to the adverse environmental impacts related to their production and use. Alternatively, biobased emulsifiers can serve such a purpose. In this regard, lignin, which is the main component of lignocelluloses materials, can be converted to emulsifiers for oil-water emulsions. In this regard, the production of lignin-based emulsifiers has not been explored comprehensively. In this thesis, lignin-derived emulsifiers were experimentally produced via polymerizing lignin and acrylic acid (AA), and its impacts on emulsions produced by mixing water and three industrially used oil of xylene, cyclo-hexane, and decane was studied comprehensively using a tensiometer, and Quartz crystal micro-balance.

It was observed that, by increasing the charge density of the kraft lignin (KL) acrylic acid polymer, KL-AA (kraft lignin- acrylic acid), its molecular weight, and carboxylic acid group were increased. The KL-AA with the highest carboxylic group, KL-AA-10, dropped the contact angle and interface tension of the emulsion more than the other KL-AA samples. Also, the emulsion containing KL-AA-10 had the highest viscosity and stability and smallest droplet size among emulsions containing other lignin derivatives. However, the lignin derivative with the lowest carboxylic acid group, KL-AA-3.5 adsorbed more than other lignin derivatives on the surface of oils.

It was also observed that decane was the least polar and thus compatible oil with water to produce an oil-water emulsion. KL-AA was generally effective for all oil-water emulsions examined in this work. However, it was more impactful on the decane water emulsion as observed via the contact angle and interface tension, viscosity, and adsorption results. The stability analysis also confirmed that KL-AA generated more stable emulsion for the decane water system than other systems.

It was also observed that the higher dosage of lignin derivatives induced more adsorption on the oil surface, which impacted the contact angle and interface tension of the emulsions more greatly and generated more stable emulsions. However, the presence of lignin aggregates at a higher lignin concentration did not improve the viscosity of the emulsion.

Author's Declaration

I, **Shirin Fatehi**, do hereby declare that I am the sole composer of this document and that this document has not been submitted, in whole or in part, in any previous application for a degree or professional qualification. This document has been authored solely by myself and is comprised of my own work, except where otherwise stated by reference or acknowledgment. I authorize Lakehead University to lend this document to other institutions and/or other individuals for academic and/or scholarly research. I further authorize Lakehead University to reproduce this document, in whole or in part, via photocopying and/or digital scanning at the request of other institutions and/or individuals for academic and/or scholarly research. I authorize Lakehead University to make this document available electronically to the public.

Shirin Fatehi

Acknowledgment

Table of Contents

List of Figures

List of Tables

Chapter 1. Introduction

1.1. Introduction

The mixture of two immiscible liquids is called emulsion that has many uses such as, cosmetic paint, textile, and food industries (Goodarzi and Zendehboudi 2019). Emulsions without emulsifiers are thermodynamically unstable systems(Wu and Ma 2016). To the immiscibility of oil and water, emulsifiers are extensible used to produce stable emulsions. However, the currently used emulsifiers are mostly produced from petroleum-based chemicals and thus environmentally unfriendly, are expensive and sometimes ineffective.

To address these challenges, biobased emulsifiers have been produced and examined as bio-emulsifiers of oil-water emulsions. Although great progress has been made in this regard, there is room to produce new impactful bio-emulsifiers for different industries.

Lignin is one of the main components of lignocelluloses materials and it has many functional groups, such as phenolic hydroxyl groups, that can participate in various reactions to produce advanced functional materials. In this regard, lignin acrylic acid polymers were produced in the last (Kong et al. 2018) and their efficiencies in flocculating particles in wastewater systems have been examined (Kong et al. 2018). Since a lignin-acrylic acid polymer has phenolic hydroxyl and carboxylic acid groups, it can interact with both water and oil and presumably can function as an emulsifier. However, the emulsifying affinity of this new material, i.e., lignin-acrylic acid, has not been evaluated yet.

This thesis contains the following succeeding chapters:

Chapter 2. *Literature review*: In this chapter, the relevant topics to the subjects of oil-water emulsions, the use of synthetic and bio-emulsifiers, and the production and use of lignin and lignin derivatives are reviewed. Also, the fundamental concepts, e.g., rheology and stability of emulsions, associated with the characteristics of emulsions, e.g., rheology and stability, are comprehensively reviewed.

Chapter 3. *Methodology*: In this chapter, the materials and experimental methodologies for generating and characterizing lignin-acrylic acid polymers, the surface and interface tension of water and oil mixtures, contact angle of water containing solutions, oil droplet size, adsorption of lignin-acrylic acid on oil, and the rheology and stability of oil-water emulsions are comprehensively explained.

Chapter 4. *Results and discussion*: In this chapter, the results for inducing lignin acrylic derivatives are presented. Then, the impacts of lignin derivatives on the surface and interface properties of oil-water emulsion, oil droplet size, rheological properties, and stability of oil-water mixtures are systematically presented using figures and tables. The results are then compared, and relevant discussion is made. The reasons for the behavior of lignin derivatives in different systems are interpreted and relevant references to support the arguments are presented.

Chapter 5. *Conclusions and recommendations*: In this chapter, the overall conclusions of this thesis work are summarized and future work to continue this research is suggested.

Chapter 6. *References:* in this chapter, the relevant references cited in this thesis are presented.

1.2. Objectives and novelty

The overall objectives of this work were to 1) study the impact of the characteristics of lignin-acrylic acid polymers on the emulsion properties of oil-water mixtures; 2) study the impact of oil type on the performance of lignin-acrylic acid as an emulsifier for the oil-water mixtures; and 3) to examine the impact of the dosage of lignin-acrylic acid on its emulsifying affinity of the polymer in different oil-water systems.

The main novelty of this work was the comprehensive examinations and thus the correlations developed between the properties of lignin-acrylic acid and the contact angle and interface tension of oil-water mixtures, the adsorption performance of lignin derivatives on the oil surface, the rheological properties of the oil-water mixture, and emulsion stability of the oil-water mixtures. These assessments were carried out for the first time, and no report is available in the literature on this topic.

Chapter 2. Literature Review

2.1. Emulsions

An emulsion is defined as the dispersion (droplets) of a liquid in an immiscible liquid. The phase that is suspended in the emulsion is called the external or continuous phase. The phase that appears in the form of droplets is the internal or dispersed phase of the emulsion. In the case of oil emulsions, one of the liquid phases is generally crude oil and the other liquid is an aqueous phase or water. Emulsions can be categorized according to the size of droplets in the continuous phase flow (Tarasov et al. 2018). The emulsion is known as a macro emulsion if the dispersed droplets are larger than 0.1 mm. Two common destabilization processes that influence the uniformity of dispersions are the migration of the particles and droplet size variation or accumulation.

The stability of the emulsions is limited by different phenomena including coalescence, flocculation, sedimentation, phase inversion, creaming, and Ostwald ripening (Fingas and Fielhouse 2004). Despite the use of many emulsifiers to produce stable emulsions, the currently used emulsifiers are synthetic and expensive materials with considerable environmental footprints. To reduce the use of such synthetic materials, efforts are under way for the production of environmentally friendly emulsifiers. For example, lignin-derived emulsion systems have been examined recently (Zembyla et al. 2020). However, current knowledge on the impact of lignin-derived emulsifiers is limited.

2.2. Formulation of emulsions

Adequate mixing and the presence of a surface-active agent are two vital factors that lead to the emulsion formation when the oil and water phases are brought together. In emulsion formulations, mixing is primarily used for evenly distributing oil and water in the systems. Generally, the larger the amount of shear, the smaller the droplet size of the dispersed phase and the tighter the emulsion (Moradi et al. 2010). However, mixing and energy use are correlated and the mixing process is not appreciated in the emulsion systems. The second most important factor in emulsion formation is the presence of an emulsifying agent. The composition and amount of the emulsifier considerably dictate the type and tightness of the emulsion.

2.3. Types of emulsions

Emulsions can be categorized into two main groups of water in oil and oil in water emulsions (Goodarzi and Zendehboudi 2019). Water-in-oil emulsions comprise water droplets in an oil-continuous phase, and oil-in-water emulsions are attributed to droplets of the oil phase in a continuous flow of water (Gellerstedt and Gustafsson 2007). The type of formed emulsions depends on a variety of factors, such as the water/oil ratio and temperature. Emulsions can also be categorized according to the size of droplets in the continuous phase flow (Goodarzi and Zendehboudi 2019). The emulsion is known as a macro emulsion if the dispersed droplets are larger than 0.1 mm. This category of emulsions is generally thermodynamically unstable as the two phases tend to coalesce and separate due to the reduction in interfacial energies over time. However, the stabilization mechanisms can eliminate the rate of droplet coalescence (Tambe and Sharma 1995). In contrast to macro-emulsions, the second category of emulsions, labeled as micro-emulsions, are formed when two immiscible fluids coexist due to their severe low-interfacial energy. The size of droplets in micro emulsions is less than 10 nm and they are considered thermodynamically stable mixtures. Micro-emulsions are generally different from macro-emulsions in terms of their stability and formation (Healy et al. 1976). Table 2.1 presents the descriptions of micro emulsions.

Table 2.1. Various categories of micro-emulsions (Urbina et al. 2000)

Micro-emulsions Type	Phase equilibria	Description
Type I	Oil-in-water (o/w)	The surfactant is usually soluble in water (Winsor I). A small concentration of soluble surfactant exists in water in the form of monomers.
Type II	Water-in-oil (w/o)	The surfactant is preferentially soluble in the oil phase. The aqueous phase is present along with an oil phase rich in the surfactant (Winsor II).
Type III	Three-phase system	Excess water and oil phase coexist with a middle phase of rich surfactant in this category (Winsor III or middle-phase micro-emulsions).

| Type IV | Micellar solution | An isotropic single-phase micellar solution forms by adding a sufficient quantity of surfactant with alcohol. |

2.4. Emulsion characteristics

To prepare a stable emulsion, the interfacial characteristics of an emulsion should be altered by emulsifiers, which are responsible for the coalescence event (Maphosa and Jideani 2018). Another criterion for a stable emulsion formation is that the droplet size should be sufficiently small so that the collision forces acting on the continuous phase molecules produce the Brownian motion, which prevents settling (Tadros 2013). Fresh emulsions can demonstrate different characteristics than aged ones. This is attributed to the variation in the oil type due to the presence of absorbable components, differences in emulsifier adsorption rate, and its ability to produce a film at the interface. When the mixture is subjected to a considerable change in the temperature or pressure, the emulsion characteristics, such as viscosity and droplet size can alter significantly (Ghosh and Rousseau 2010). The emulsifying agents are developed to stabilize emulsions. They are classified into two types: finely divided solids; and surface-active agent (Binks et al. 1999). Fine solids generally stabilize emulsions mechanically. These materials, which are wetted by both water and oil, should be smaller than the emulsion droplets and should accumulate at the water/oil interface. The effectiveness of these particles in stabilizing emulsions is strongly dependent on various factors, such as inter-particle interactions, particle size, and wettability of the material. Fine solid materials existing in the produced oil include clay particles, sand, asphaltene/wax, silt, and mineral scales deposited on the water/oil interface (Mclean and Kilpatrick 1997; Urbina-Villalba 2009). Surface-active agents or surfactants are the particles that are soluble in both oil and water phases. They have a hydrophilic branch, which has a tendency to interact with oil, and there is a hydrophobic branch that has an affinity towards water. Surfactants tend to create an interfacial film at the oil-water interface (Schramm et al. 2003). This phenomenon generally leads to a reduction in the interfacial tension (IFT) and, consequently enhances the droplet dispersion and emulsification.

2.5. Mechanism of emulsifiers

From a thermodynamic perspective, an emulsion is an unstable system due to its natural tendency for a liquid/liquid mixture to minimize its interfacial interactions (and/or interfacial energies)

(Alinezhad et al. 2010). Oil-field emulsions are usually categorized based on their degree of kinetic stability. The interactions between the surface-active agents and water/oil interfaces are primarily responsible for emulsion stability. Following the first drop formation, the former emulsion begins to be altered due to various time-dependent processes, which are Ostwald ripening, coalescence, flocculation, sedimentation, and creaming (the most controversial processes) (Mohammed et al. 1994). Stabilizing mechanisms are that water/oil emulsions are assumed to be liquid/liquid colloidal dispersions. Their kinetic stability is a result of droplets of small size and the formation of an interfacial layer between the water and the oil droplet. Emulsion stabilization is improved by emulsifier injection as a consequence of electrostatic and steric forces.

The stabilization of water-oil emulsions produced from oil fields occurs through the formation of a thin film at the interface of the suspended droplets in the continuous phase. These films increase the emulsion stability by increasing the viscosity of the interfacial film (Raya et al. 2020). The viscous interfacial films reduce the drainage rate of the film during the water droplets, coalescence by creating a repulsive barrier, which consequently lowers the emulsion breakdown rate (Costa et al. 2019). The properties of interfacial films depend on several factors, such as polar molecules, concentration in the heavy oil, crude oil type (asphaltic and paraffinic), aging time, temperature, and pH and composition of the water phase (Bonto et al. 2019).

Table 2.2. Demulsification mechanisms of water-oil and oil-water emulsions (Wang et al. 2021)

Demulsification process	Definition	Details
Sedimentation	- Water droplets falling from an emulsion, which normally occurs due to the difference in water and oil density (Walstra 2005)	- It is a function of a chemical structure and surfactant adsorption. - due to the difference in oil and water density
Creaming	- Not an actual breaking, but the separation of an emulsion into the denser part (cream) and the other parts	- It is a function of a chemical structure and surfactant adsorption. - due to the difference in oil and water density

Flocculation	- It exhibits grouping of individual suspended droplets together while each droplet keeps its identity	- It depends on the surfactant structure. - It is the first step towards further emulsion aging and coalescence. - More frequent mechanisms in oil/water emulsions.
Coalescence	- It represents the mechanism by which two or more separate groups of miscible particles are active as they pull each other to reach the slightest contact.	- It is affected by the interfacial film viscosity, surfactant film elasticity, and the dynamics of thin liquid film drainage.
Aggregation	- It corresponds to the formation of accumulated droplets in a suspension.	- It is the most common process, resulting in the destabilization of colloidal systems.
Ostwald ripening	- It represents the diffusion of droplets into the continuous phase to describe the inhomogeneous structure modification such as the redeposition of surfactant particles into larger particles over time.	- Generally experienced in water/oil emulsions. - It is observed in liquid droplets or solid solutions.
Phase separation	- It is defined as a complete separation of oil and water into two distinct phases.	- It is a function of time and emulsifier type.

2.6. Surfactants

Surfactants are commonly used as emulsifiers in oil-water emulsions as they interact with both oil and water and stabilize the oil-water systems. Surfactants are substances that have hydrophobic and hydrophilic groups. The hydrophobic group does not show affinity to water, but the hydrophilic group has an affinity to water. Surfactants are classified into ionic surfactants and nonionic

surfactants. Ionic surfactants are sub-classified into anionic surfactants where the hydrophilic group dissociates into anions in aqueous solutions, cationic surfactants that dissociate into cations, and amphoteric surfactants that dissociate into anions and cations often depending on the pH. Nonionic surfactants are surfactants that do not dissociate into ions in aqueous solutions, and they are subclassified depending on the type of their hydrophilic group. Common hydrophilic groups of ionic surfactants are carboxylate ($-COO-$), sulfate ($-OSO_3-$), sulfonate (SO_3-), carboxybetaine ($-NR_2CH_2COO-$), sulfobetaine ($-N(CH_3)_2C_3H_6SO_3-$), and quaternary ammonium ($-R_4N+$). In an aqueous solution, the carboxylate anion forms a structure with counterions, such as Na^+, K^+, or Mg^{2+}. The hydrophilic group of nonionic surfactants is usually a polyoxyethylene group, but there are also nonionic surfactants with glyceryl groups or sorbitol groups, and nonionic surfactants with these different hydrophilic groups are also used depending on the application (Nakama 2017).

2.7. Lignin
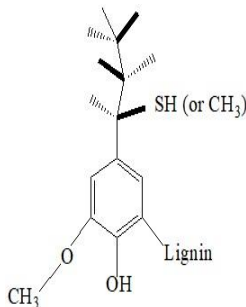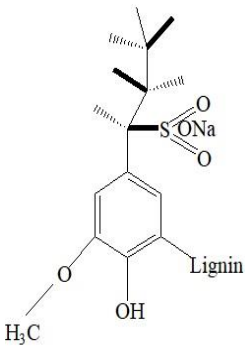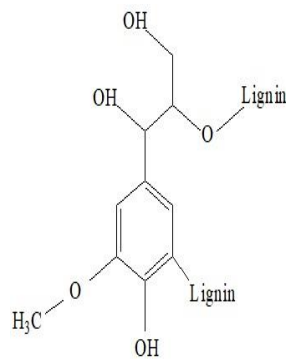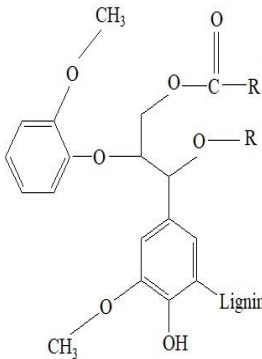
Lignin is a heterogeneous and unshaped polymer that makes a large portion of the cell wall of vascular plants, making it the second most sample biomass on earth just after cellulose (Liu et al. 2018). The main role of lignin is to provide rigidity to strengthen the structure of cell walls. It also contributes to water transport and the protection of cell walls against biological stresses. The lignin of various species contains three main units of monolignols. Based on the types of plants (softwood, hardwood, and non-wood), the amount of each monolignol could be different. Lignin extracted from softwood resources merely contains coniferyl alcohol monolignols. The lignin of hardwood contains the highest amount of syringyl alcohol among the three classes of lignin with a smaller amount of coniferyl alcohol monolignols. Lignin can be isolated from the spent liquors of kraft, sulfite, soda, and organosolv pulping processes. Among these, sulfite and kraft processes are the two dominant techniques that are commercially utilized in the pulping industry (Vishtal and Kraslawski 2011; Tarasov et al. 2018). Lignin produced from the kraft process is usually used as a fuel and burned in mills, while lignin generated in the sulfite pulping process is extracted as lignosulfonate. The solubility of kraft lignin is much lower than that of lignosulfonate due to the lack of hydrophilic groups on its structure. There is considerable room for taking great advantage of the inherent potential of lignin for value-added applications. However, a small fraction of extracted lignin is currently used in the formulation of adhesive (Liu and Li 2007) dispersants (Zhou et al. 2006), surfactants, or as antioxidants in rubbers and plastics (Laurichesse and Avérous 2014;

Saraf and Glasser 1984). This implies that lignin valorization has not been fully explored and there is considerable room for generating value-added products, such as lignin-derived emulsifiers.

2.8. Lignin Structure

Lignin has a large and complex polymeric structure containing methoxyl groups, phenolic hydroxyl groups, and some terminal aldehyde groups in the side chain (Liu et al. 2015). It is commonly distributed in combination with hemicellulose around the cellulose strands in primary and secondary cell walls of cellulose fibers, and it is covalently bound to the carbohydrate/cellulose structure (Galkin and Samet 2016; Zakzeski et al. 2010). Table 2.3 summarized the structures and properties of the four technical lignin.

Table 2.3. Technical lignin and their properties (Gellerstedt and Gustafsson 2007)

Technical lignin	Kraft	Lignosulfonate	Soda	Organosolv
Structure				
Separation methods	Precipitation (pH change)	Ultrafiltration	Precipitation (pH change) Ultrafiltration	Precipitation (addition of non-solvent) Dissolved air flotation
Product status	Industrial	Industrial	Industrial	Laboratory/Pilot
Sulphur (%)	1.0 to 3.0	3.5 to 8.0	0	0
Nitrogen (%)	0.05	0.02	0.2 to 1.0	0 to 0.3
Molecular weight ($\times 10^3$ g/mol)	1.5 to 5 (up to 25)	1 to 50 (up to 150)	0.8 to 3 (up to 15)	1.5 to 2.5

Polydis-persity	2.5 to 3.5	6 to 8	2.5 to 3.5	1.5 to 2.5
Acid solu-ble lignin (%)	1 to 5	-	1 to 11	~2
Solubility	Alkali, some organic solvents (DMF, pyridine)	Water	Alkali	Wide range of organic solvents

2.9. Dominant pulping processes

2.9.1. Kraft process

Kraft pulping is the dominant method used for processing lignocellulosic biomass, and it accounts for roughly 85% of the produced lignin in the world (Xu et al. 2014). In the conventional kraft process, the delignification process is performed at high temperatures and pH, during which lignin is dissolved in the pulping liquors (Azadi et al. 2013; Doherty et al. 2011). In these pulping processes, lignin is dissolved by the cleavage of the ether linkages at pH between 13 and 14 and temperatures around 170°C, which would increase the number of phenolic hydroxyl groups of lignin allowing its solubilization at high pH in the pulping liquor. From this liquor, lignin can be isolated via acidification (e.g., sulfuric acid) at a pH of 5–7.5 (Azadi et al. 2013).

2.9.2. Sulfite Process

The sulfite process is an old pulping method for pulp and paper production. This process involves the reaction between lignin and a metal sulfite and sulfur dioxide, with calcium, magnesium, or sodium acting as counter ions available in the pulping chemicals (Doherty et al. 2011). By changing the conditions of the pulping process and chemical dosage, the pH of the pulping system can range between 2 and 12. The process is executed at temperatures that can vary between 120 and 180°C, with a digestion time of 1–5 h (Azadi et al. 2013; Saake and Lehnen 2007).

2.10. Potential application of lignin

Lignin can be used as a starting material for producing different materials. Generally, lignin-based materials can be used mainly as fuels, chemicals reagents, and polymers.

For example, lignin can be used for fertilizer and herbicide productions used in agriculture, as dispersant agents, sizing agents in the paper industry, and as binders in plywood manufacturing (Chakar and Ragauskas 2004; Galkin and Samet 2016; Zakzeski et al. 2010). Lignin and its derivatives have been used in composites, resins, and as flocculants, dispersants UV blocking agents, and for medical purposes.

2.10.1. Lignin for composites

Lignin can be used as a reinforcing polymer for composite production. However, it is always a big challenge to develop miscible lignin/polymer composites, as raw lignin is not well miscible or compatible with many polymers, especially in non-polar systems. The poor interfacial binding between lignin particles and the polymer matrix tends to favor particle aggregation and phase separation in the resultant blends (Kai et al. 2016).

2.10.2. Lignin for phenol-formaldehyde resins

Phenol-formaldehyde (PF) resins are a class of synthetic polymers with excellent mechanical strength, good heat and moisture resistance, and advanced ablative properties (Galkin and Samet 2016). With such advantages, PF resins have been widely used for various applications in electronics, railway, building, and construction products as coatings, insulation, lamination, wood bonding, and well known as plywood adhesives (Azadfar et al. 2015; Tejado et al. 2007).

2.10.3. Lignin as ultraviolet (UV) blocking agent

During lignin production in pulping processes, lignin chromophores are generated that are UV absorbant. Recently, the use of lignin-derived materials as a UV blocking agent in various applications, such as cosmetics and sunscreen creams were reported (Chaochanchaikul et al. 2012).

2.10.4. Lignin for biomedical applications

There have been reports on the use of lignin-based antibacterial and anticancer agents for various applications (Figueiredo et al. 2018). Generally, the carboxylic acid, phenolic hydroxyl, and chro-

mophore structures of lignin contribute to their application in the medical field. Also, various lignin derivatives, such as oxidized lignin (Liu et al. 2019), have shown promising results as anti-cancer materials (Azadfar et al. 2015; Chaochanchaikul et al. 2012; Fernandes et al. 2013).

2.10.5. Lignin as flocculants

Recently, the production and application of lignin derivatives as flocculants for various solutions and suspension systems were studied (Gao et al. 2021). As lignin is generally water-insoluble, lignin was made soluble via polymerization for large molecular weight flocculant generation. Polymerization was the main procedure to produce high molecular weight lignin for flocculant production. Altered cationic and anionic lignin polymers were produced under alkaline and acidic conditions and in solvent systems (Henrikki Sipponen et al. 2017). Reports are available on their effectiveness as flocculants for municipal and industrial wastewater, kaolin and aluminum oxide suspensions, and dye-containing solutions (Guo et al. 2018; Wang et al. 2018; Wu and Ma 2016).

2.10.6. Lignin as dispersants

Oxidation, sulfoalkylation, and carboxyalkylation have been utilized comprehensibly to induce lignin-derived dispersants (Chen et al. 2018; He et al. 2017). The reports generally concluded that carboxyalkylated (Konduri et al. 2015) and oxidized lignin is an effective dispersant for the suspension system, but its effectiveness is pH-dependent, and its efficiency drops at pH below 4, as carboxylic acid groups are protonated at low pH. However, sulfoalkylated lignin (Hopa and Fatehi 2020) showed promising results that were independent of pH.

2.11. Impact of lignin properties on its performance

Correlations between the properties and performance of lignin-derived materials are available in several research publications (Chen et al. 2018). It was reported that the degree of oxidation affected the performance of oxidized lignin as flocculant for dye solution (He et al. 2016), and for cement admixture (He et al. 2015). The degree of sulfonation has also impacted the performance of sulfonated lignin as cement dispersants (Chen et al. 2018).

Also, the impacts of charge density (Konduri and Fatehi 2018) and molecular weight (Tolbert et al. 2014) of lignin polymers on their flocculation performance for kaolin (Hasan and Fatehi 2018) and aluminum oxide (Kazzaz et al. 2018) suspensions were reported in the past.

As lignin-acrylic acid polymers with different molecular weights and charge densities can be produced via polymerizing lignin and acrylic acid (Kong et al. 2018), it is also important to explore the impact of the molecular weight/charge density of lignin-acrylic polymers on its emulsifying performance in the oil-water mixtures. This investigation will help with the design of lignin-acrylic acid emulsifiers for altered oil-water emulsion systems.

2.12. Methodology Fundamentals

2.12.1. Contact angle and interfacial analysis

The surface tension of lignin-containing solutions was determined to understand how lignin derivatives would change the surface properties of water and thus its interaction with oil (Alwadani et al. 2021). The measurement was conducted by the Du Noüy ring method. In this method, a platinum ring is submerged below the surface of lignin-containing water and pulled up gradually, which pulls the water surface upward. The maximum tension that water can tolerate the pulping is considered as the surface tension of lignin-containing water (Ghavidel and Fatehi 2021).

The water contact angle of lignin-containing water was also determined following the sessile drop method that relies on the contact angle of a water droplet and a solid surface, in this thesis, glass slides.

The oil contact angle (OCA) of the three-phase system was also determined following the method discussed in a previous thesis (Ghavidel 2021). In this method, a glass slide that contains lignin-containing water droplets were submerged into the oil, and the contact angles of a solid surface at an oil-water interface the slides were determined as shows in Figure 2.1.
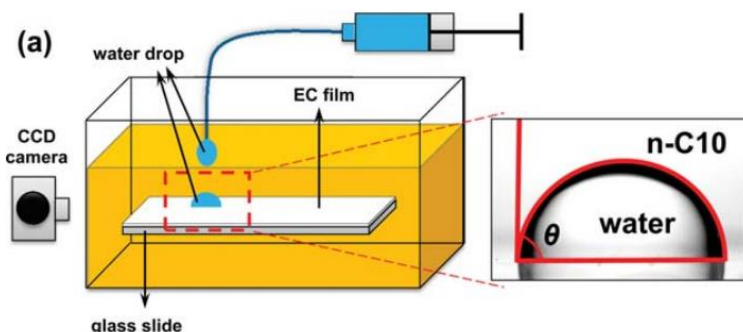
Figure 2.1. Illustration of oil-water contact angle measurement (Ghavidel 2021).

2.12.2. Adsorption analysis

Quartz crystal microbalance with dissipation (QCM-D) technique was used in this thesis as a sensitive tool for investigating the adsorption of lignin-acrylic acid polymers on oil surfaces. QCM relies on the oscillation of a quartz crystal sensor at a frequency provided by an external voltage. In addition to the adsorbed mass shown based on changes in frequency of the quartz crystal, structural (viscoelastic) properties of adsorbed layers can also be investigated via monitoring changes in the dissipation parameter (D). Dissipation occurs when the voltage to the crystal is turned off and the energy from the oscillating crystal dissipates from the system.

The oscillating crystal with the changes in voltage is shown in Figure 2.2a. The high sensitivity of the instrument is associated with the repetition of voltage changes (voltage is applied and turned off) over 100 times per second. Figure 2.2b shows the signal generated by an oscillating crystal and the differences in signal decay between rigid and viscoelastic materials.
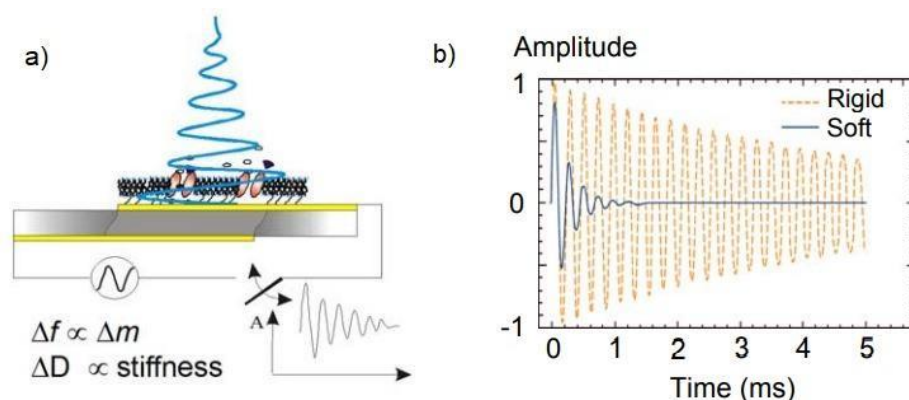
Figure 2.2. a) The oscillating crystal when voltage is applied on the sensor and shear wave penetrates the adsorbed layer, b) the different dissipations for rigid and soft adsorbed layer (Ghavidel 2021).

2.12.3. Rheology analysis

Rheology is the study of the flow of matter, the science of deformation and flow within a material. It applies to a material that has a complex microstructure such as muds, sludges, suspensions, polymers, and other glass forms, as well as biological, and other materials that belong to the class of soft matter such as food. It depends on the complex behavior of viscoelasticity of materials that have the properties of both liquids and solids relying on the forces/deformations applied to them.

Rheology generally explains the behavior of Newtonian and non-Newtonian fluids, by characterizing the minimum number of functions that are needed to relate stresses-strain.

In this thesis, the viscosity of oil-water emulsions was studied comprehensively. Viscosity can be conceptualized as quantifying the internal frictional force that arises between be the side of layers of fluid that are in relative motion. This analysis is important as it shows how oil-water emulsion moves on the macroscopic scale and how the droplets of emulsion are stabilized in emulsion systems. Generally, high viscosity is required to stabilize the forces developed between droplets in emulsion and thus to keep the emulsion stabilized. Otherwise, a low viscosity promotes the movement of droplets and coalescence.

In addition to yield stress for viscosity measurement, an amplitude sweep test was also carried out, which is based on an oscillatory assay that applies an increasing amplitude (i.e., energy input) to probe sample characteristics, such as rheological stability. In this work, I applied this method to understand how strong the emulsions are stable.

2.12.4. Stability analysis

The stability of the emulsion systems was studied using a vertical scan analyzer. The samples were prepared inside the glass container of the instrument and subjected to analysis. The sample was scanned with a pulsed near-infrared light ($\lambda = 880$ nm) and the transmitted and backscattered lights were recorded by the detectors of the instrument in which a microscopic fingerprint of the samples could be recorded. The stability of samples was quantitively analyzed by terms of stability index (TSI), where both coalescence and settling phenomena are considered in TSI evaluation. The TSI is determined by equation 2.1.

$$TSI = \sqrt{\frac{\sum_{i-1}^{n} (x_i - x_{bs})^2}{n-1}} \qquad (2.1)$$

Where n, xi, xbs, refer to the number of scanning, an average of the backscattered light intensity at the scanning time, and an average of xi, respectively. The higher the TSI, the lower the stability is (Xu et al. 2018).

Chapter 3. Experimental Methods

3.1. Materials

Softwood kraft lignin (KL) produced via the LignoForce™ technology was received from FPIn-novations. Also, acrylic acid (AA), potassium persulfate ($K_2S_2O_8$), sodium hydroxide (NaOH, 97%), sulfuric acid (H_2SO_4, 98%), dimethyl sulfoxide-d_6 (DMSO-d_6), cyclohexane (C_6H_{12}), deuterium oxide (D_2O), acrylic acid (AA), n-decane ($C_{10}H_{22}$), polydiallyldimethyl-ammounium chloride (PDADMAC, 100,000-200,000 g/mol), potassium hydroxide (0.8N), para-hydroxy benzoic acid (0.5%), KCL (1M) and cellulose membrane tubes (1000 g/mol cut off) were purchased from Sigma-Aldrich. Xylene ($C_6H_6(CH_3)_2$ ≥98.5%, ACS grade as a mixture of ortho, meta, and para isomers, cyclohexane (99%), and decane (99%) were purchased from Fisher Scientific. All chemicals were used without further purification. HPLC-grade water was produced by a Milli-Q water purifier and used in the QCM and Zeta potential experiments.

3.2. Polymerization of kraft lignin with acrylic acid

The reaction was performed in 500 mL three-neck flasks under a nitrogen atmosphere equipped with magnet stirrers. First, 4 g of lignin were suspended in 20 mL of deionized water at room temperature and stirred at 300 rpm for an hour. While stirring, the different amounts of AA were added to the flasks, and the balance was made with deionized water to make the reaction solution 40 mL. After deaeration, the solution was transferred to a preheated water bath at 80°C. After 5 min, the preheated (80°C) amount of initiator ($K_2S_2O_8$, 1.5 wt.%) was added to the flasks to initiate the reaction at 300 rpm. After 3 h, of reaction at pH 3, the reaction was quenched, and the pH of the reaction was adjusted to 1.5 to precipitate the KL-AA polymer product from the solution. Then, the reaction system was centrifuged to precipitate KL-AA polymer from PAA homopolymer and unreacted AA monomer. The solution was then dialyzed using membrane tubes for 2 days to remove impurities and AA monomers. Then, the samples were dried in an oven at 105 °C (Kong et al. 2018). The polymerization reaction was repeated under different amounts of AA to lignin molar ratios (3.5, 7.5, and 10). The products of this analysis were called KL-AA-3.5, KL-AA-7.5, and KL-AA-10, respectively, in this thesis.

3.3. H-NMR analysis

The chemical structure of KL and KL-AA polymer was analyzed with ^{1}H-NMR. In this set of experiments, 70 mg of KL was dissolved in 1 mL of DMSO, and 70 mg of KL-AA was dissolved in 1 mL of D$_2$O. The solution was stirred overnight to fully dissolve the lignin derivatives. The ^{1}H-NMR spectra and two-dimensional homonuclear correlation spectroscopy spectrum (COSY) were obtained using nuclear magnetic resonance spectroscopy (AVANCE NEO-1.2 GHz, Bruker, Corporation). Adjustments for ^{1}H-NMR and COSY are as follows: ^{1}H-NMR: 64 number of scans, A 90° pulse with a relaxation delay of 1.00 s; ^{1}H–^{1}H COSY: 4 scans per increment with 128 increments, A 90° pulse with a relaxation delay of 1.00 s.

3.4. Solubility, charge density, and carboxylic acid group analyses

At first, a 1 wt.% solution of lignin samples was prepared via mixing the lignin samples with deionized water at room temperature. The solutions were shaken for 1 h at 100 rpm at 30°C. After shaking, the solutions were centrifuged at 1000 rpm for 5 min to separate the soluble part of lignin derivatives from the solutions.

For measuring the solubility, after filtering the solution, the dried weight of insoluble lignin derivatives left on the filter was determined, which helped determine the solubility of the lignin samples via developing mass balance. The filtrate part of the solution was taken for the charge density analysis of soluble lignin. The charge density of soluble lignin samples was determined via direct titration, using a Particle Charge Detector, Mutek PCD-04 titrator (Herrsching, Germany) and with PDADMAC or PVSK standard solutions (~0.005 mol/L)(Inwood, Pakzad, and Fatehi 2018). The carboxylic acid group and phenolic of KL and KL-AA polymers were measured using an automatic potentiometric titrator (785 DMP Titrino, Metrohm, Switzerland). About 0.06 g of dried KL and KL-AA polymers were added to 100 mL of deionized water containing 1 mL of 0.8 mol/L potassium hydroxide in a 250 mL beaker. After stirring at 200 rpm for 5 min, 4 mL of 0.5 % para-hydroxybenzoic acid solution was added as an internal standard, and the solution was titrated with 0.1 mol/L hydrochloric acid solution. During the titration, with the decrease in the pH of the sample solutions, three endpoints appeared in sequence (V1', V2' and V3', respectively). The corresponding three endpoints in the titration curve of the blank sample (i.e., sample without lignin) were quantified as V1, V2, and V3, respectively. The carboxylic acid and phenolic hydroxyl contents of samples were calculated according to equations (3.1) and (3.2) (Kong et al. 2018).

Phenolic hydroxyl group $(\frac{mmol}{g})= \frac{C_{HCl}\,[(V_2'-V_1')-(V_2-V_1)]}{m}$ (3.1)

Carboxylic acid group $(\frac{mmol}{g})= \frac{C_{HCl}\,[(V_3'-V_2')-(V_3-V_2)]}{m}$ (3.2)

where C_{HCl} is the concentration of HCl solution (0.1 mmol/L) as the titrant, m is the mass (g) of the sample. V_1, V_2, and V_3 are the volumes (mL) of HCl solution consumed for the three endpoints in blank titration. $V_{1'}$, $V_{2'}$, and $V_{3'}$ are the volumes (mL) of HCl solution consumed for the three endpoints in sample titration, respectively. Results are the average of three repetitions.

3.5. Molecular weight analysis

The molecular weight of samples was determined using a Gel Permeation Chromatography system, Malvern GPCmax VE2001 Module + Viscotek TDA305 with multi-detectors (UV, RI, viscometer, low angle, and right-angle laser detectors). For KL measurement, the columns of PAS106M, PAS103, and PAS102.5 were used and tetrahydrofuran (THF) with a fixed flow rate of 1.0 mL/min was used as eluent and solvent. For KL-AA polymer measurement, the columns of PAA206 and PAA203 were used, and $NaNO_3$ solution (50 g/L) was used as solvent and eluent at the fixed flow rate of 0.1 mol/L. Poly (ethylene oxide) was used as a standard polymer in the GPC measurement. An average of 3 independent measurements was reported in this work.

3.6. Surface tension and contact angle

 For surface tension measurements, 2.5 wt.% KL-AA solutions were diluted to generate 2, 1.5, 1, 1.125, 0.75 and 0.56 wt.% solutions. The surface tension of the solutions was measured following the Du Nouy ring method ring (Sigma 701, Biolin Scientific) and using OneAttension software at room temperature. In detail, the small vessel (30 mL) of the instrument was washed with deionized water, and the Du Nouy ring was cleaned with a lighter for 5 seconds before each test. Then, 20 mL of the lignin solutions were placed into the small vessel, and the test was conducted for 10 points. The data generated in this test was used for identifying the critical aggregation concentration (CAC) of lignin samples and the results were calculated from the average of 10 independent measurements.

For the contact angle measurement, the two-phase water contact angle (WCA) and three-phase oil contact angle (OCA) were determined using a theta optical tensiometer attention (Biolin Scientific). First, a 300 µL of KL-AA solution at different concentrations of (1, 2 wt.%) were coated on clean glass slides using a spin coater (WS-400B-NPP) spin-processor (Laurell Technologies Corp) at 1500 rpm and the acceleration rate of 200 m/s^2 for 20 sec under nitrogen environment. The coated films were dried in the oven at 105°C overnight. Then, a drop of deionized (DI) water (5 µL) was placed on the coated glass slides, and the contact angle of KL-AA at the water-air interface (WCA) was determined following static contact angle (i.e., two-phase contact angle) measurement via the sessile drop method at 25 °C for 10 sec (Ghavidel and Fatehi 2019). Afterward, the slides were transferred to a glass chamber filled with 3 mL of organic solvents solvent (i.e., xylene, cyclohexane, decane) to reproduce the situation, in which emulsification occurs when KL-AA polymers are spread in water first and then interacted with oil interface.

3.7. Dynamic interfacial tension

Dynamic interfacial tension (γ) between KL-AA of different concentrations and the organic phases was determined using an Attension Theta Biolin optical tensiometer following the pendant drop method (Bizmark and Ioannidis 2017). In detail, 3 mL of xylene, cyclohexane, decane oils was poured into a Quartz cuvette and sealed to minimize the volume loss. In this test, 5 µL droplets of KL-AA solutions (1 and 2 wt.%) were generated at the tip of a needle, which was submerged into the oil phase (Bi et al. 2015). The images of the droplets were recorded over 3600 s at a frame rate of 10 images per second in the first 600 sec and 1 image per minute in the last 3600 s. The interfacial tensions were calculated from the analysis of the shape of droplets using the Young-Laplace equation (Pan et al. 2018).

3.8. Zeta potential

The zeta potential of the KL-AA solution was determined using a NanoBrook PALS (Brookhaven Inc., USA). KL-AA solutions with different concentrations (1 and 2 wt.%) were prepared via stirring at 300 rpm and 25°C overnight. Afterward, 250 µL of potassium chloride was added to 1 L MiliQ water and stirred for 30 min. Then, 20 mL of KCl solution was filtrated and used in this measurement. Afterward, 50 µL of KL-AA solutions were added to 50 mL of the filtrated KCl and

sonicated for 15 seconds. The zeta potential analysis was executed at room temperature and a constant electric field of 8.4 V/cm. The reported data was the average of three repetitions.

3.9. QCM-D measurements

The QCM measurement was conducted with 3 solvents of xylene, cyclohexane, and decane coated on an aluminum oxide sensor (QSX-309) and the solutions (0.05 wt.%) of KL-AA. As the aluminum oxide sensor was positively charged and our KL-AA and oil samples were negatively charged, we chose this sensor for analysis to have sensible adsorption. First, the sensors were cleaned via sonicating in 99 vol% ethanol for 15 minutes. Then, the sensors were dried with nitrogen and then treated with UV/ozone (PSD Series, digital UV ozone system, NOVASCAN) for 15 min. Afterward, xylene, cyclohexane, and decane (5 µL) were coated on sensors at 3000 rpm for 30 sec under N_2 environment at the acceleration rate of 200 m s^{-2} (Ghavidel and Fatehi 2020), separately. Then, the sensors were dried in an oven at 110 °C for 30 minutes. The coating procedure was repeated 10 consecutive times while drying the sensors in the oven between each coating cycle. The QCM-D measurement started by rinsing the sensors with the buffer solution of MilliQ water until a baseline was stabilized. Then, the buffer solution was changed to KL-AA (0.05 wt.%), and the experiment was carried out at the flow rate of 0.15 mL/min and room temperature using Quartz crystal microbalance with dissipation (QCM-D 401, E1, Q-Sense Inc. Gothenborg, Sweden). The experiments were conducted for 20 min, after which the analysis was finished by rinsing the sensors with the buffer solution.

3.10. Emulsion preparation

First, KL-AA solutions with 1 and 2 wt.% concentrations were prepared. Then, they were mixed with xylene, cyclohexane, and decane as the organic phase at the 1/1 volumetric ratio in clean glass vials. Then, the mixtures were emulsified using an ultrasonic machine (Omni-Ruptor 4000, Omni International Int.) at room temperature, 240 W power, and 30 s for 3 sec intervals.

3.11. Rheology properties

The emulsions of lignin-AA were generated as stated earlier. A hybrid rheometer (TA Instruments) equipped with a cylindrical geometry (cone diameter, 28.03 mm; cone length, 41.96; angle, 1°;

gap, 5500 µm) at room temperature for determining the viscosity and other rheological properties of the emulsions. Precisely, 1 mL of each emulsion was transferred by a pipet onto the lower plate of the instrument. To determine the linear viscoelastic region of KL-AA, an amplitude sweep test was performed in the range of 0.1 and 100 1/s at a frequency of 10 rad/s. A strain of 10% was chosen from the linear viscoelastic region to carry out frequency sweep measurements in the range of 0.1 and 1000 rad/s. For the oscillation amplitude test, the strain of 0.1-100% with a constant frequency at 10 rad/s was chosen to determine the storage and loos modulus of the emulsions.

3.12. Stability analysis

The solutions of KL-AA solutions at 1 and 2 wt.% concentrations were prepared. Then, 6 mL of KL-AA emulsions were prepared via mixing 2 mL of KL-AA and 3 mL of oils in glass vials. The emulsions were formed by ultrasonication at 240 W power and 30 s with 3 s time intervals. Then, they were mixed with a vortex mixer (VWR) at 2500 rpm for 10 s. After mixing, they were placed in a vertical scan analyzer (Turbiscan Lab Expert, Formulation, France), at room temperature for 24 h.

3.13. Visual analysis

Emulsions of KL-AA and oil (6 mL) were prepared as stated above. The structure of the emulsions was immediately analyzed by a Leica TCC-SP8 confocal laser scanning microscope (Leica Microsystems Inc., Germany) equipped with a WLL laser (563 nm excitation wavelengths) using an HC PL APO CS2 100×/1.40 oil immersion objective lens. First, 40 µL of emulsions without dilution were taken from the emulsion layer of the samples immediately after the preparation. The emulsions were placed on glass slides with cover glass slides on the top. Red fluorescence was used for observation of the samples with a 600-710 nm filter under a 563 nm laser illumination.

Chapter 4. Results and Discussion

4.1. Lignin-acrylic acid properties

It was previously reported that the polymerization of KL and AA was optimized at 1.5 wt.% initiator (potassium persulfate), 80℃ and 3 h, which were selected in the current analysis (Kong et al. 2018). Water-soluble lignin-acrylic acid (KL-AA) polymers were produced with different molecular weights. Table 4.1 lists the properties of KL-AA polymers. It is obvious that the KL-AA with a higher charge density and the carboxylic acid group had a higher molecular weight. It can be observed that by changing the AA/lignin molar ratio from 3.5 to 10, the molecular weight increased rapidly from 3.07×10^5 to 7.99×10^5 g/mol, the charge density was increased from 1.1 mmol/g to 4.7 mmol/g and the carboxylic acid groups were increased from 1.09 mmol/g to 2.23 mmol/g. Such increases were attributed to the improved polymerization of lignin and AA as the amount of AA in the system was increased (Witono et al. 2012). In another research on KL-AA production (Kong et al. 2018), water-soluble KL-AA was produced at neutral pH. Generally, the polymerization mechanism of KL and AA under acidic conditions is encouraged by the decomposition of the initiator (Kong et al. 2018). Also, more PAA chains would be grafted on KL under acidic conditions than alkaline (Kong et al. 2018). The phenolic group of KL was originally 3.26 mmol/g, but it decreased to 1.58, 1.64, and 1.76 mmol/g after polymerization with AA, these results would imply that the KL and AA polymerization mainly occurred on the phenolic group of KL (Kong et al. 2018). The self-decomposition of potassium persulfate in the initiator system generates sulfate radicals (Hunkeler 1991) and the sulfate radicals can remove hydrogen from the hydroxyl groups on lignin and generate lignin macro radicals. Once the macromolecular radicals are generated, they react with the monomers and initiate the polymerization (Mondal and Haque 2007; Panesar et al. 2013). Although the solubility of KL was improved via polymerization with AA, the KL-AA samples were partially water soluble. In another report (Gao et al. 2021), lignin was sulfonated before polymerizing with AA to improve the water solubility of the KL-AA product. Furthermore, when the polymerization of KL-AA was accelerated, its hydrogen and carbon decreased, which is associated with the addition of the carboxylic acid group to KL (Petridis et al. 2011).

Table 4.1. Properties of KL and KL-AA

Sample	KL	KL-AA-3.5	KL-AA-7.5	KL-AA-10
lignin concentration, wt.%	4	4	4	4
Time (h)	-	3	3	3
Temperature (°C)	-	80	80	80
AA/lignin molar ratio	-	3.5	7.5	10
Solubility (wt.%)	9.6	52.9	73.7	91.6
Charge Density (mmol/g)	0.1	1.1	2.2	4.7
M_w, $\times 10^5$ (g/mol)	2.13	3.07	6.11	7.99
M_n, $\times 10^5$ (g/mol)	1.46	1.52	1.54	2.04
M_w/M_n	1.58	2.0	3.9	3.9
carboxylate group, mmol/g	0.83	1.09	1.37	2.23
Phenolic hydroxyl group, mmol/g	3.26	1.57	1.12	0.84
Carbon, (wt.%)	64	60	58	50
Hydrogen, (wt.%)	7.0	1.3	3.2	5.8
Oxygen, (wt.%)	27	35	36	44

4.2. H-NMR discussion

The NMR spectroscopy analysis permitted us to obtain the structural characterization of the KL-AA. Figure 4.1a shows the H-NMR spectra of KL and KL-AA polymers. The peak in the range of 6-7.5 ppm attributes to the hydrogen in the phenolic hydroxyl group of lignin (f in Figures 4.1a and 4.1.b). Moreover, in all samples (KL-AA-3.5-KL-AA-7.5 and KL-AA-10), the peak at 3-3.9 ppm is attributed to the protons in methoxyl groups and the peak at 1.4-2.4 ppm is for the protons of CH_2, CH, and COOH of lignin-acrylic acid. Peaks that appeared at 4.5-4.9 ppm are assigned to the solvent of D_2O. It can be observed that the peaks for the KL-AA chain segment appeared at 1.1 ppm, 1.9 ppm, and 2.4 ppm, that the peaks appeared at 1.1 ppm is attributed to C-1(a), at 1.9

ppm is attributed to C-2(b), that are attributed to presence of acrylic acid and 2.4 ppm is assigned to the carboxylic acid of PAA(c) (Petridis et al. 2011). The peaks at 2.50 ppm, 3.2-3.9 ppm, and 6.5-7.1 ppm on the KL-AA spectrum belonging to KL illustrate the successful polymerization of KL and AA. Similarly, the peaks at 3.20 ppm, 2.55-3.0 ppm, 5.15-5.75 ppm, 5.99-7.42 ppm, 8.30 ppm, and 9.2 ppm belonging to KL illustrate the successful polymerization of KL and AA. In all samples (KL-AA-3.5, KL-AA-7.5, and KL-AA-10), the peaks range were the same, but, by increasing the ratio of AA/KL, we can observe larger peaks for AA in the spectrum of KL-AA. In another word, the KL-AA sample with a higher AA had a larger peak for ($-CH_2-O-C_6H_5-n$) (1.5-2.5 ppm). Also, the peak at 4.10 ppm in KL-AA samples is assigned to the protons of $-CH_2-$ (d in the figure) connected to the aromatic structure through ester bond ($-CH_2-O-C_6H_5$). The 2D-COSY spectra of KL and KL-AA-10 depicted in Figure 4.1c were used for confirming the signal assignments of KL-AA. In this analysis, long-range coupling of protons can be observed via considering long analysis times and the cross-peaks (not on the diagonal) that are symmetric to the crosswise COSY spectra. As seen in (Figure 4.1.a), despite the detected overlapping areas in the 1D spectrum of sample KL-AA-10, the diagonal-signal peak detected in 2D spectra at 4.50 and 1.2-2.6 ppm confirms the presence of acrylic acid in the structure of the KL-AA.
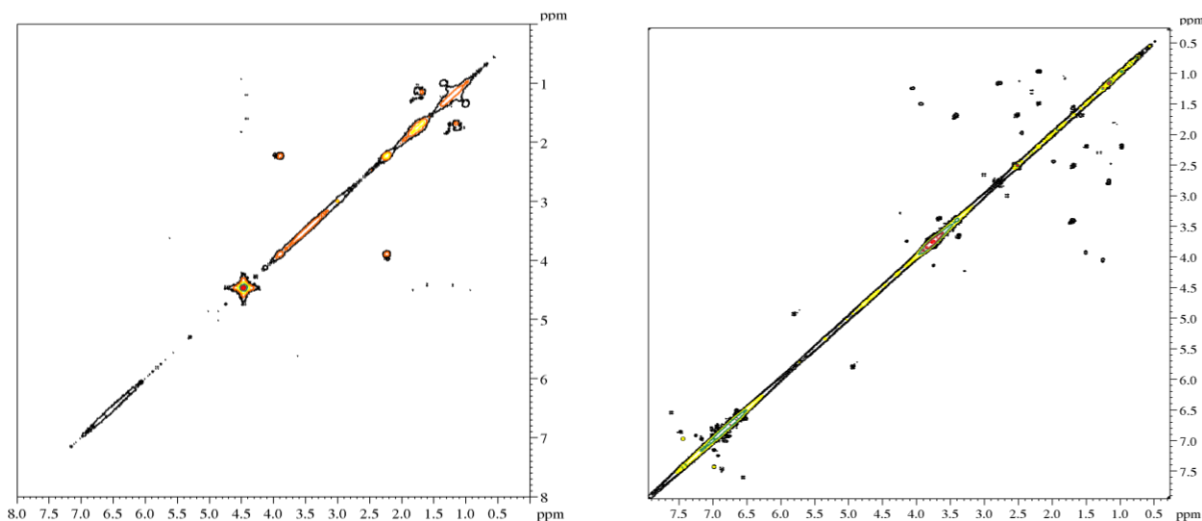
a
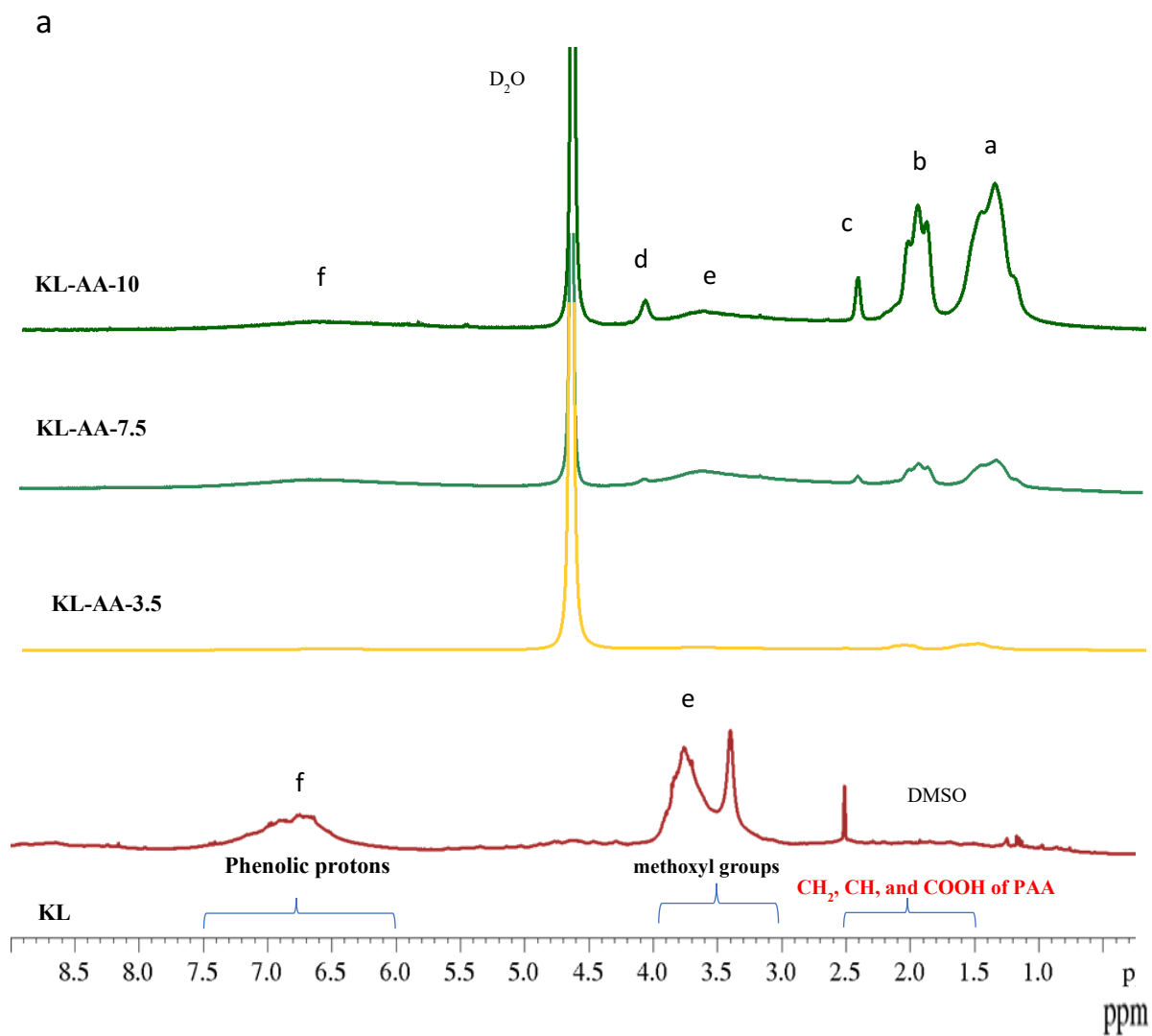
b
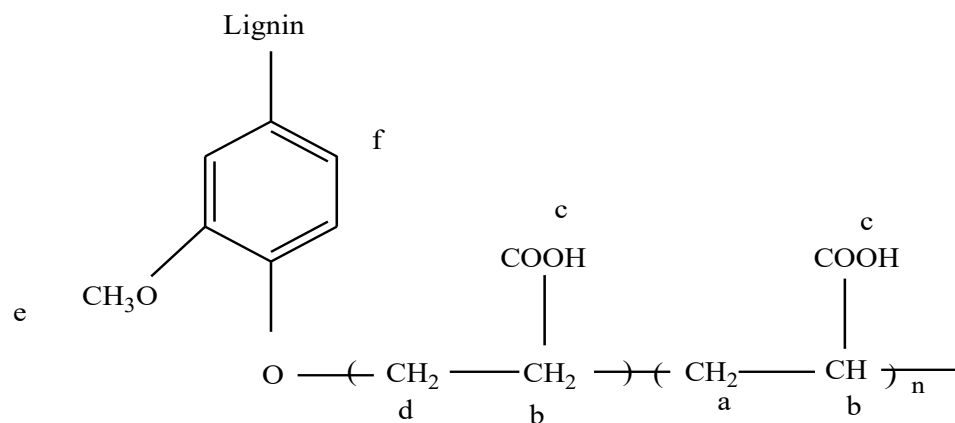
c

Figure 4.1.a) ^{1}H-NMR of lignin derivatives, b) chemical structure of KL-AA, and c)^{1}H–^{1}H COSY spectra of KL (right) and KL-AA-10 (left)

4.3. Zeta potential discussion

The stability of the samples depends on the repulsive and attractive forces between the particles in the solutions, and the presence of high repulsion between particles introduces particle stability (Nune et al. 2009). Figure 4.2 shows a slight increase in the value of ζ from approximately zero to -58 mV for KL-AA-3.5, from -to -60 for KL-AA-7.5, and -62 mV for KL-AA-10 when the dosage of KL-AA increased 2 wt.%, respectively. The higher zeta potential and thus electrostatic repulsion among the polymer segments in KL-AA solutions originating from the carboxylic acid group affected the zeta potential more significantly, which would eventually impact the stability of emulsions (Czaikoski et al. 2020).
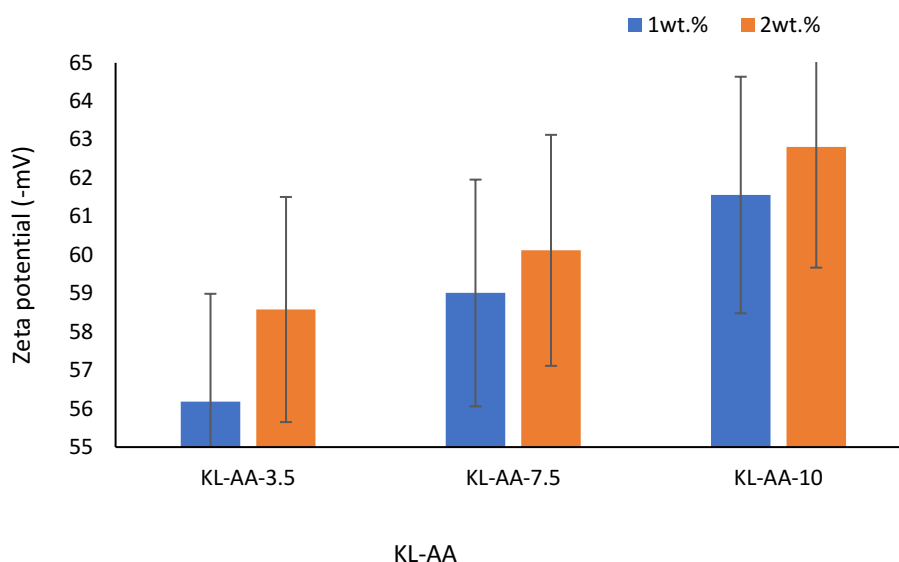
Figure 4.2. The effect of concentration on zeta potential (ζ) of aqueous solutions of KL-AA-3.5, KL-AA-7.5, and KL-AA-10

4.4. Surface tension and critical aggregation concentration

The critical aggregation concentration of 2 samples of KL-AA-3.5 and KL-AA-10 was measured with a Du Nouy ring to determine the changes in the surface tension of lignin-containing solutions and to determine the CAC point of water at an elevated concentration of the lignin derivatives for identifying the CAC point of KL-AA in an aqueous system. The results showed that the critical aggregation for both samples was at 1.5 wt.% (Figure 4.3a and 4.3b). These results imply that KL-AA would be covering the surface of the water at a 1 wt.% concentration. However, they would cover the surface of the water and make self-aggregate in water at 2 wt.%. Therefore, 1 wt.% and 2 wt.% concentrations were chosen for this further investigation to understand how different concentrations, and thus configurations of lignin particles in solution, would impact the oil-water emulsions. a concentration below and after this concentration was chosen for analysis (Ghavidel and Fatehi 2020). In another report on the surface tension analysis of kraft lignin-tannic-acid (KL–TA), the surface tension of water was 72.8 mN/m, and with an increase in the concentration of KL–TA, the molecules spontaneously adsorbed on the surface, reducing the surface tension of water in this report the tension of water was measured to be 69 mN/m, (Gharehkhani et al. 2019). In the present work, the surface tension of water was determined to be 71 mN/m, and it by adding

KL-AA because of the dissociation of carboxylate groups in water (Figure 4.3) (Gharehkhani et al. 2019). Also, by increasing the concentration of KL-AA, the surface tension dropped more remarkably for KL-AA-10 than the other sample as it has more carboxylic acid group and solubility in water (Table 4.1).
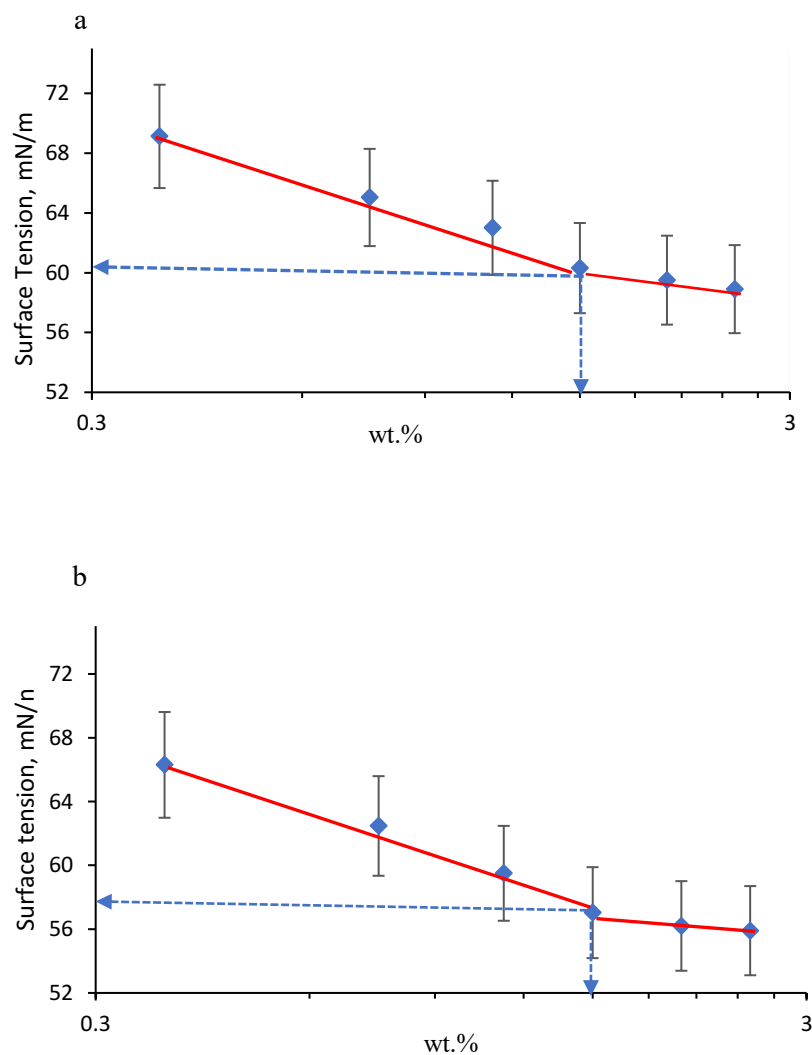

Figure 4.3. a) Surface tension of KL-AA-3.5 and b) KL-AA-10 as a function of concentration to determine CAC point.

4.5. Dynamic interfacial tension results

One of the fundamental quantities related to the assembly properties of adsorbed materials at interfaces is interfacial tension (γ). It plays a crucial role in the process of emulsion formation and stabilization (Garbin et al. 2012). Polymeric surfactants reduce γ by migrating to the interface before their concentration reaches equilibrium at the interface. In this experiment, the interfacial tension (γ) was measured following the pendant drop method with different concentrations of KL-AA (1,2 wt.%) over 3600 sec. Figure 4.4 shows the interface tension of control oil/water systems. In this figure, we can observe that xylene has the lowest interfacial tension of control oil/water systems. In this figure, we can observe that xylene has the lowest interfacial tension between 2 phases of (water and xylene) because of the high polarity of xylene in comparison with the other oil (i.e., decane and cyclohexane). Also, the rate of decline in γ varied over time, while changes were steeper in the first 250 s of the test, and it reached a plateau at the later stage of analysis (Xu et al. 2018), which is attributed to the higher polarity of the xylene at the interface (Bergfreund et al. 2019).
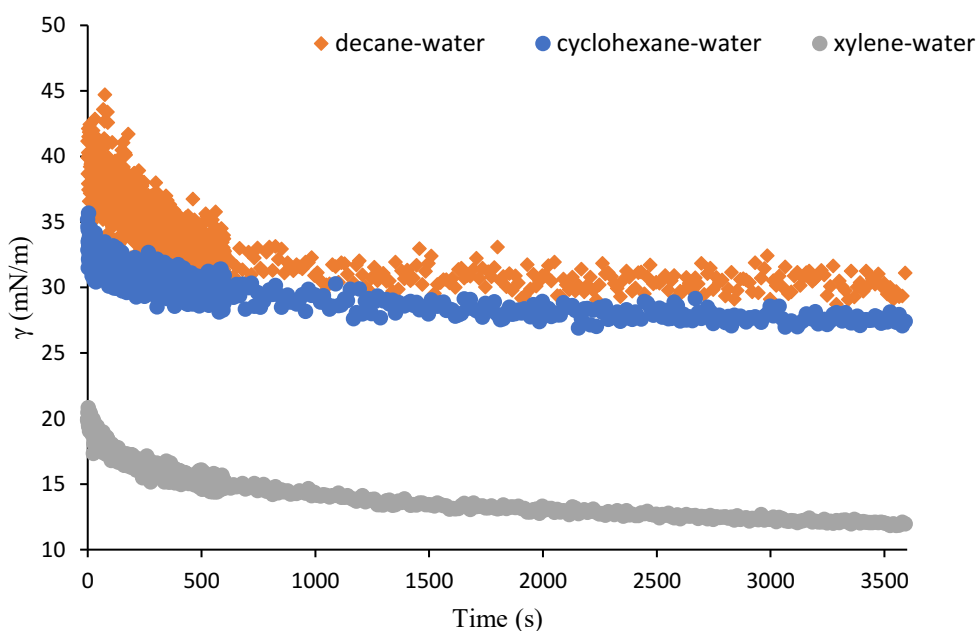

Figure 4.4. The reference baseline for the γ of the oil-water systems in the absence of KL-AA polymers

Figure 4.5 shows the interface tension of KL-AA samples at different concentrations in the three different solvents of xylene, cyclohexane, and decane. As expected, the higher concentration of KL-AA in the solution reduced its interfacial tension (γ) more greatly (Figure 4.5). As also seen, the interface tension was the lowest for the xylene-water system (Figure 4.5a), which follows the trend for the control samples in (Figure 4.4). Also, the rate of interface tension drop varied over time, while the changes were steeper in the first 250 s of the test, and it reached a plateau at the later stage of analysis, which suggests that the KL-AA deposition on the interface reached equilibrium (Bizmark and Ioannidis 2017; Wu and Honciuc 2018). The rate of interface tension drop was more significant for the xylene/water system than other emulsions, which may imply the more compatibility of KL-AA and xylene in this system. Also, the overall interface tension drops and the rate of such drops were smaller for the cyclohexane-water system implying that KL-AA was the least effective for this system. It is also noticible that KL affected the surface tension the least, and KL-AA-10 with a higher carboxylic acid group dropped the surface tnesion more siginificantly (Figure 4.5).

b

c

d

KL ■ KL-AA-3.5 ● KL-AA-7.5 ● KL-AA-10 ●

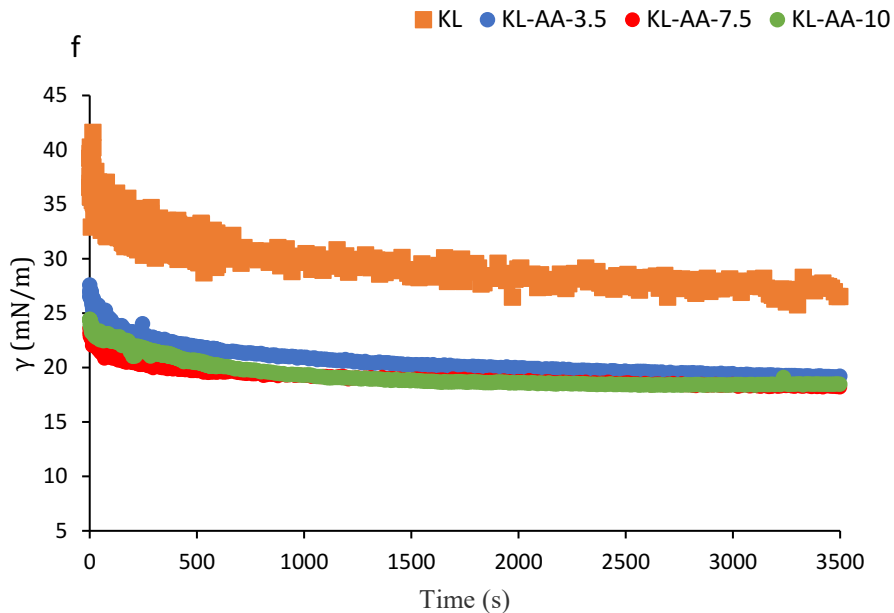e

KL ■ KL-AA-3.5 ● KL-AA-7.5 ● KL-AA-10 ●
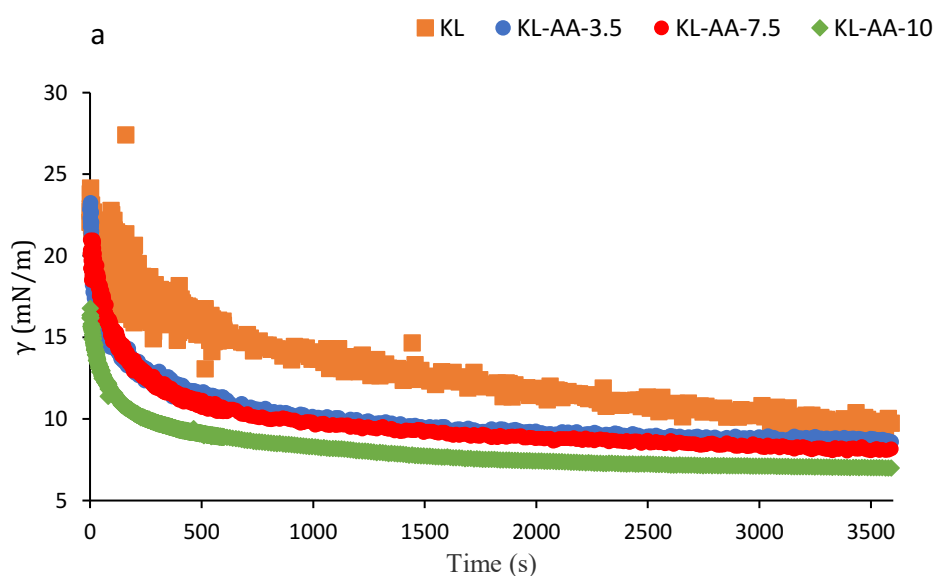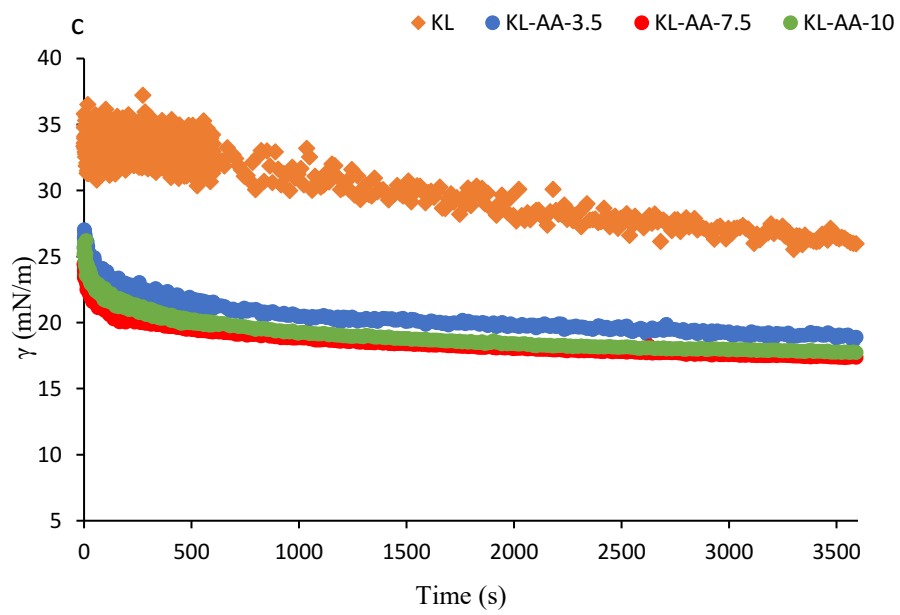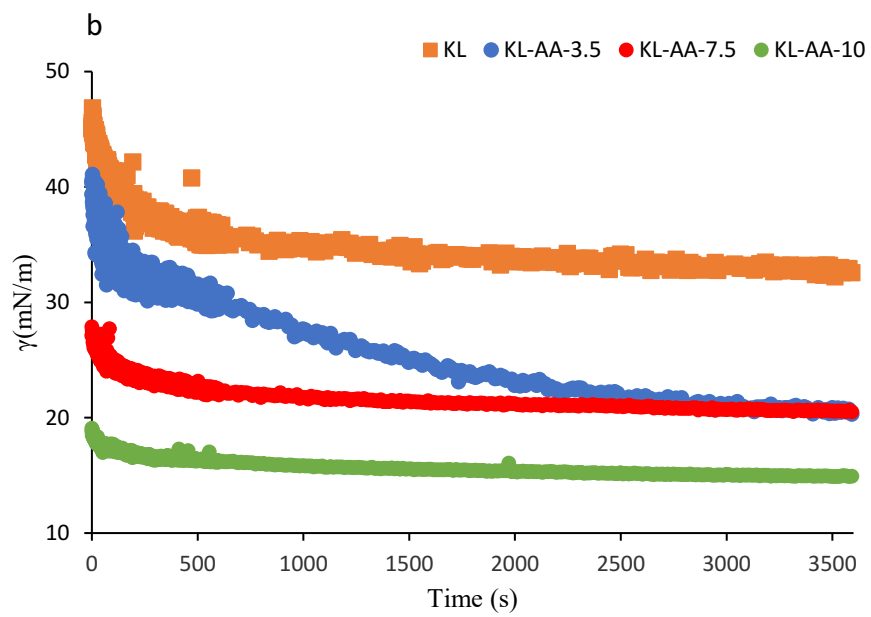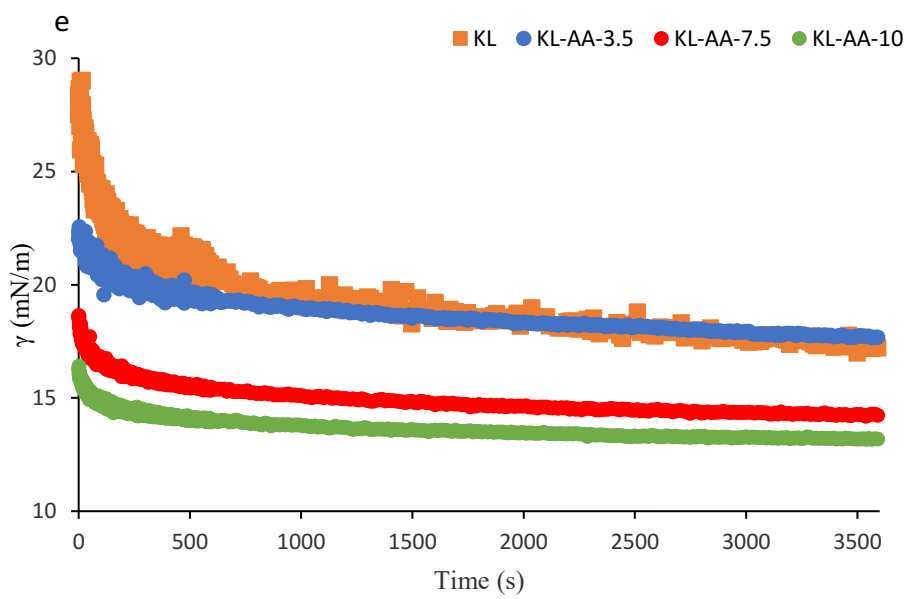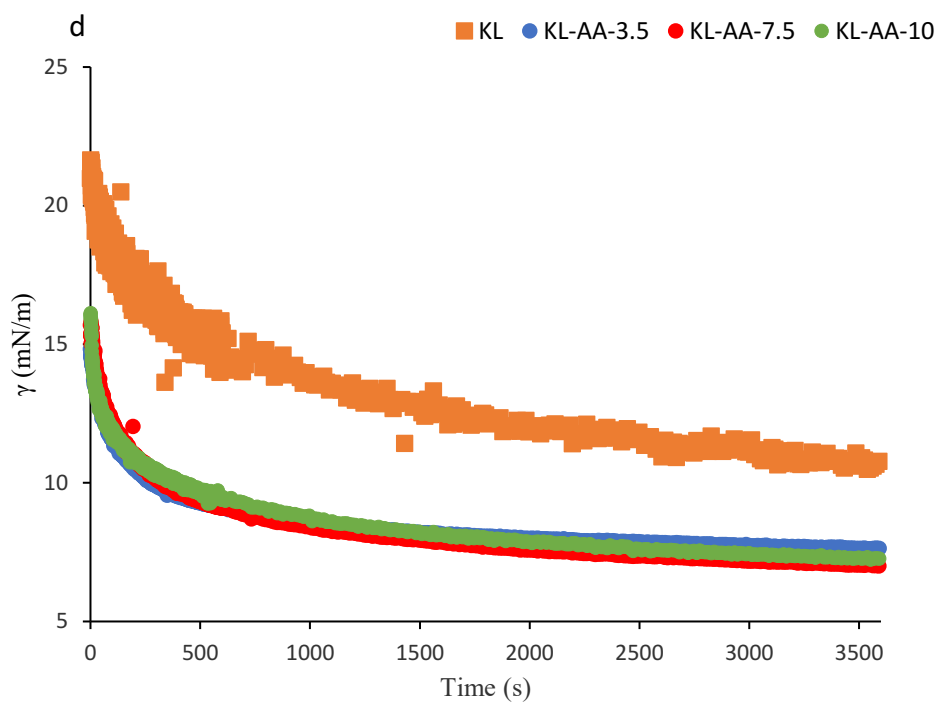
Figure 4.5. Interfacial tension (γ) of KL-AA polymers at 1 wt.% concentration for a) xylene, b) cyclohexane, c) decane, and at 2 wt.% concentration for d) xylene, e) cyclohexane and f) decane

4.6. Lignin acrylic acid diffusion into the oil-water interface

The three types of adsorption kinetics for polymers at interfaces have been reported to be diffusion-controlled, energy-barrier controlled, or a mixed barrier-diffusion (Aksenenko et al. 1998). It is generally accepted that the adsorption process at the pristine interface is diffusion-controlled when there is no energy barrier (Ghavidel and Fatehi 2021). In this case, polymer molecules easily migrate from the bulk to the pristine interface and freely adsorb. In this work, the modified Ward and Tordai diffusion model (Fainerman et al. 1994) were implemented to identify the diffusion of KL-AA from the bulk system (i.e., water) to the interface of oil-water. Assuming the adsorption barrier is not significant at the pristine interface, equation (3) can be applied as previously used for polymers and proteins. The adsorption process is characterized by $D^{*}_{t \to 0}$, effective diffusion coefficient in a short time ($t \to 0$), in which a single KL-AA polymer is adsorbed onto a free interface (Ghavidel and Fatehi 2021):

$$\gamma = \gamma_0 - 2nRTC_0 \sqrt{\frac{D^{*}_{t \to 0}}{\pi}} \times \sqrt{t} \qquad (4.3)$$

From the above equation, γ and γ_0 are the dynamic interfacial tensions at time t and pristine inter-face, respectively, n is 1 for non-ionic polymers and 2 for ionic ones. C_0 is the KL-AA concentra-tion in the solution (i.e., water, mol/L), T is the temperature, and R is the universal gas constant (8.314 J /mol. K). The changes in γ vs $\sqrt{t}$ in the initial time ($\sqrt{t} = 15\ \sqrt{s}$) for all systems is shown in Figure 4.6. Remarkably, we detected two distinguishable straight lines of γ against $\sqrt{t}$ as shown for the early stages of adsorption. While the changes of γ in the first stage are small (t→0), a larger slope of γ vs $\sqrt{t}$ was observed for the second stage (t→t1). The transition between two stages hap-pens sooner for KL-AA at the decane interface than other interfaces. Accordingly, $D^*_{t \to 0}$ and $D^*_{t \to t1}$ are obtained following equation 4.3 using the slope of a plot of γ vs $\sqrt{t}$ from Figure 3.6 for both stages (Tan and McClements 2021).
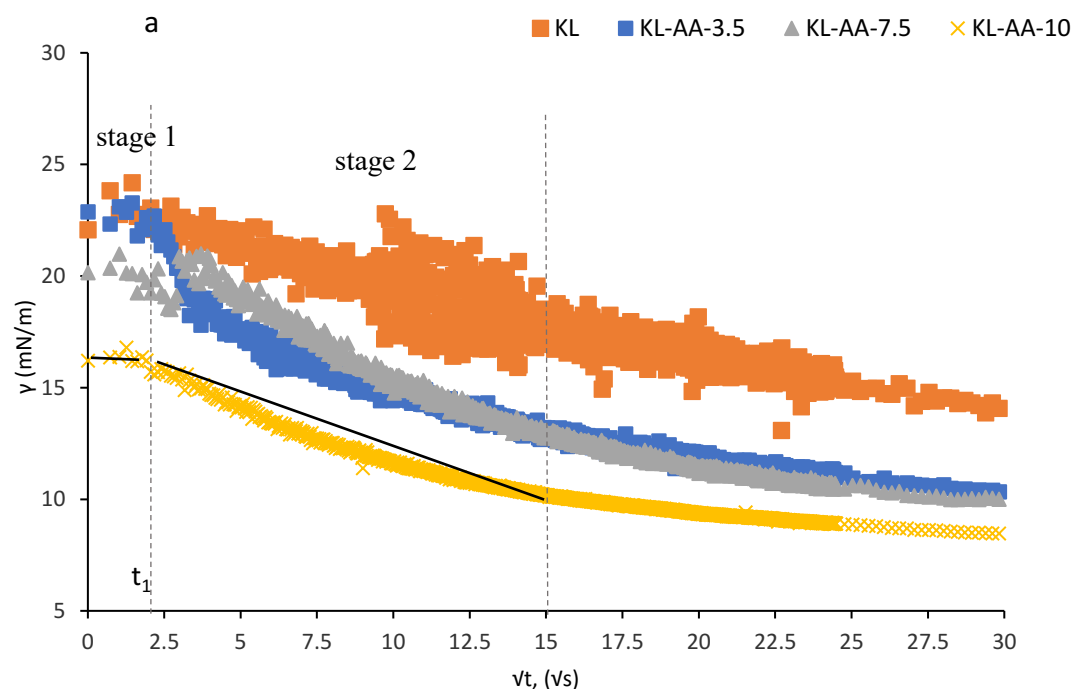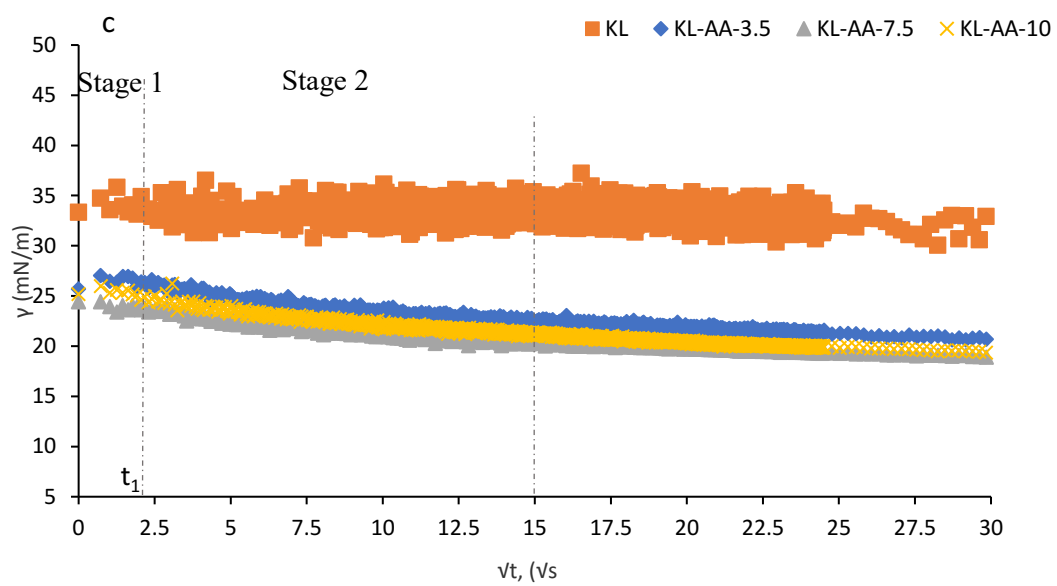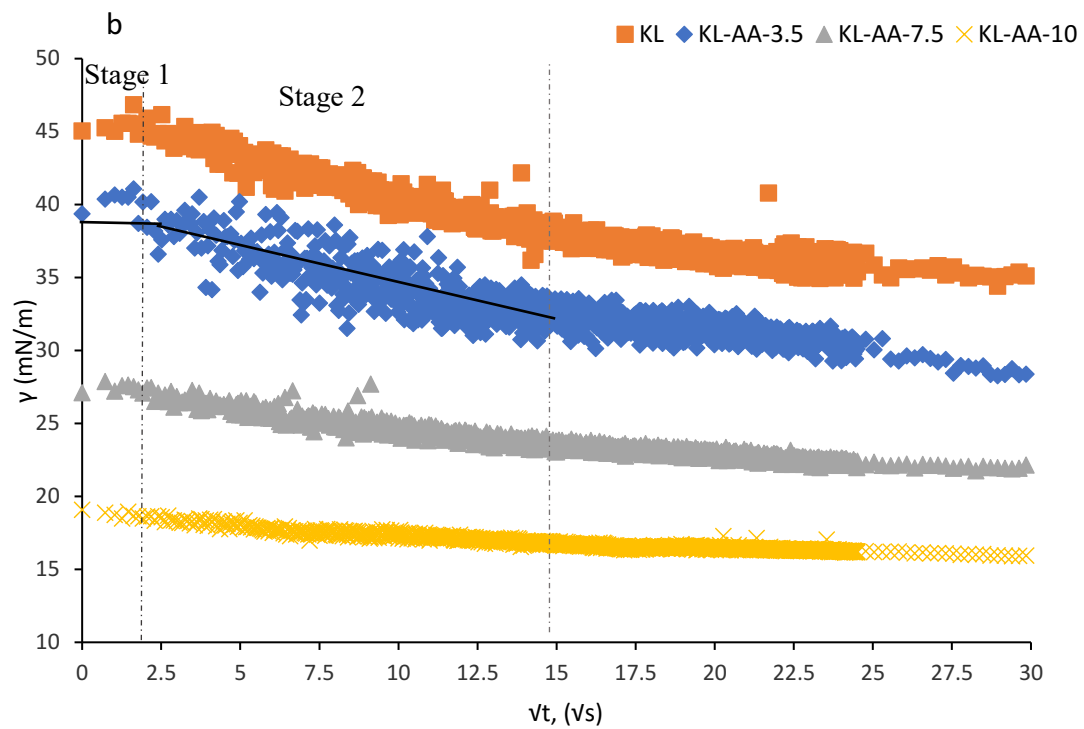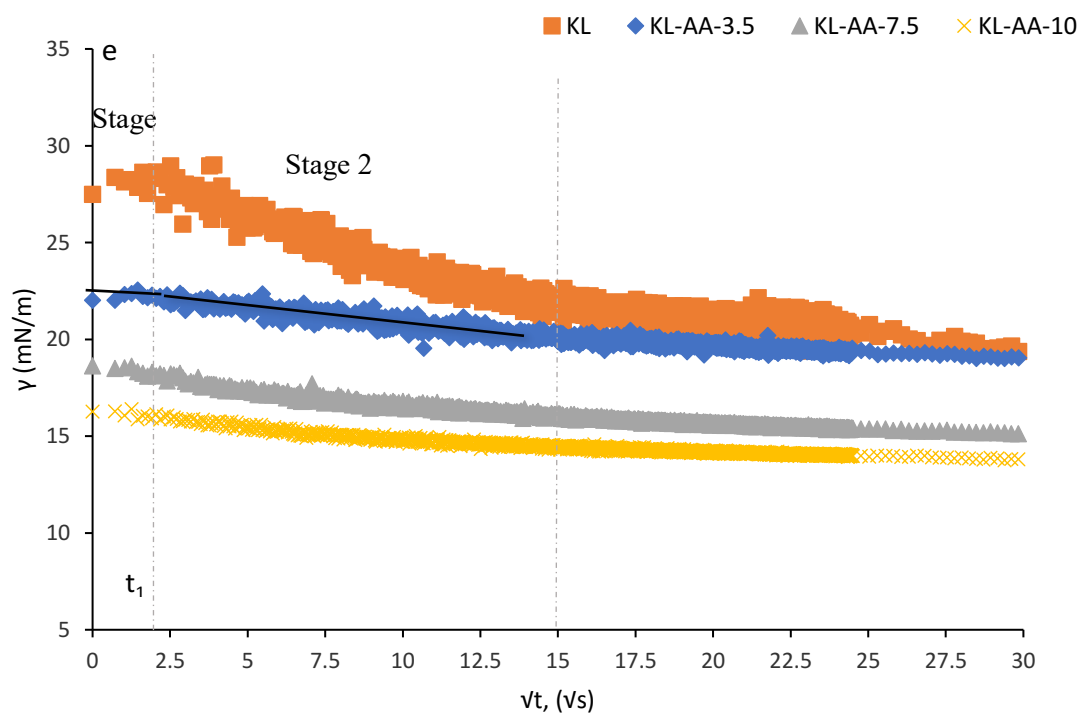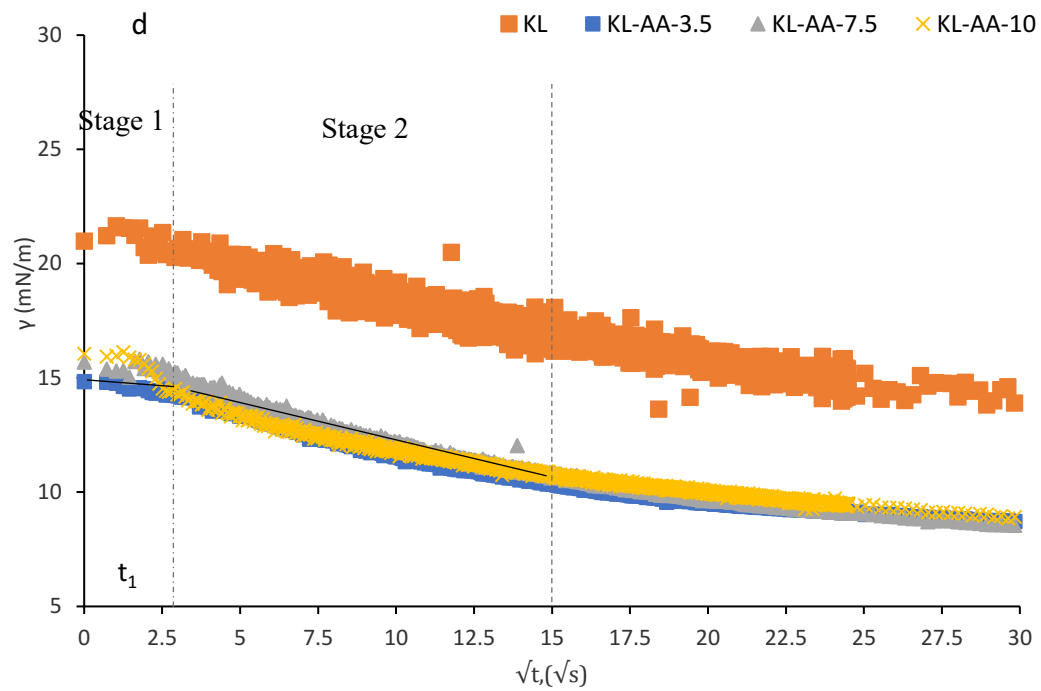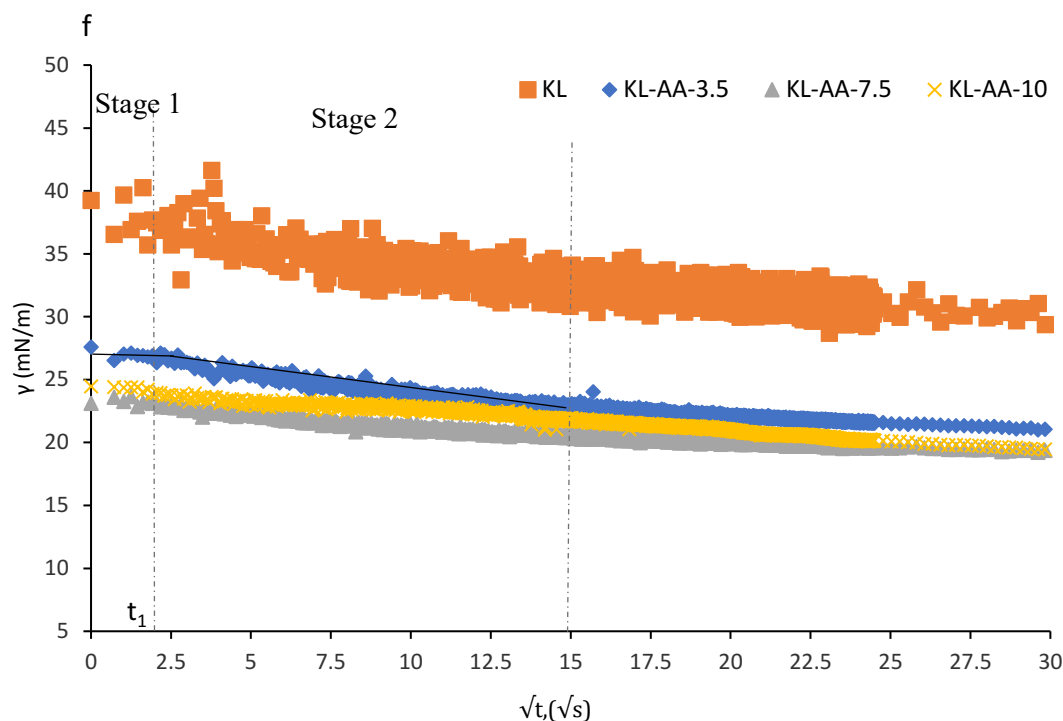
Figure 4.6. Plots of γ vs $\sqrt{t}$ showing different stages of interfacial depletion of KL-AA polymers at xylene, cyclohexane, and decane at 1 wt.% concentration of a) xylene, b) cyclohexane, c) decane, and 2 wt.% concentration for d) xylene, e) cyclohexane and f) decane

Figure 4.7 a and 4.7b show the diffusion coefficient of KL-AA-3.5 an KL-AA-10 into the interface of oil-water. These two polymers were selected as they acted as emulsifiers, and they generated different interface tensions (Figure 4.6). It is observable that KL-AA-3.5 had slower diffusion than KL-AA-10 into the interface at both concentrations of 1 and 2 wt.%. These results suggest that the lignin polymer with higher carboxylic acid group and molecular weight had higher tendency for adsorption on the interface. The higher functionality of this polymer would induce such behavior (Table 4.1). Also, the diffusion of KL-AA-10 into the interface of decane was more than that into the interface of xylene, as KL-AA-10 was more compatible with this oil due to its lower polarity.

As time elapsed, the diffusion of KL-AA-10 into the decane-water interface dropped, while that of KL-AA-3.5 into the xylene-water interface was increased (Figure 4.7c and 4.7d). The decrease in the diffusion of KL-AA-10 may be related to the repulsion force created between the already adsorbed KL-AA-10 segment at the interface and approaching KL-AA-10 segment to the interface.

The increase in the adsorption of KL-AA-3.5 on the xylene interface is related to the smaller size of this polymer that promotes its higher overall adsorption at the interface.

Also, the diffusion was slower at higher concentration (i.e., 2 wt.%) at both stages implying that self-aggregated lignin derivatives (Figure 4.3) had slower diffusion into the interface (Figure 4.7).
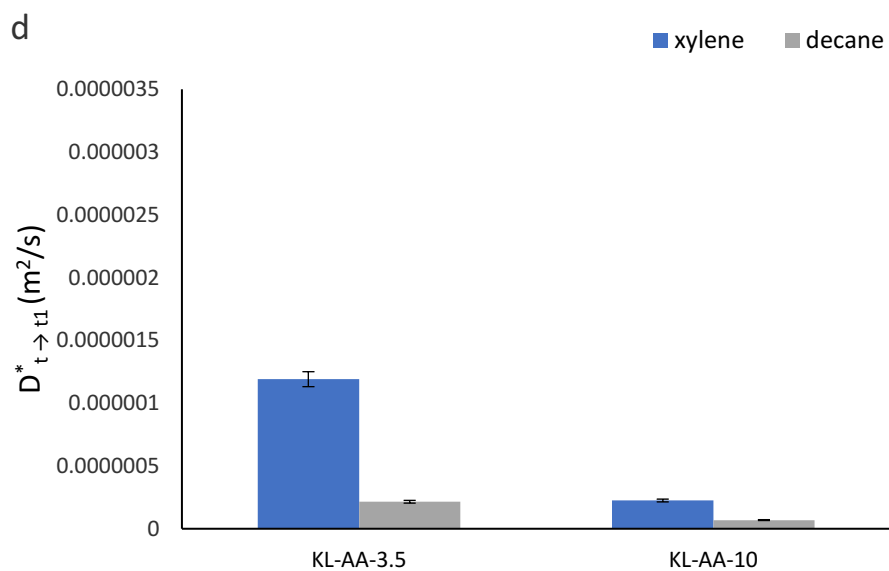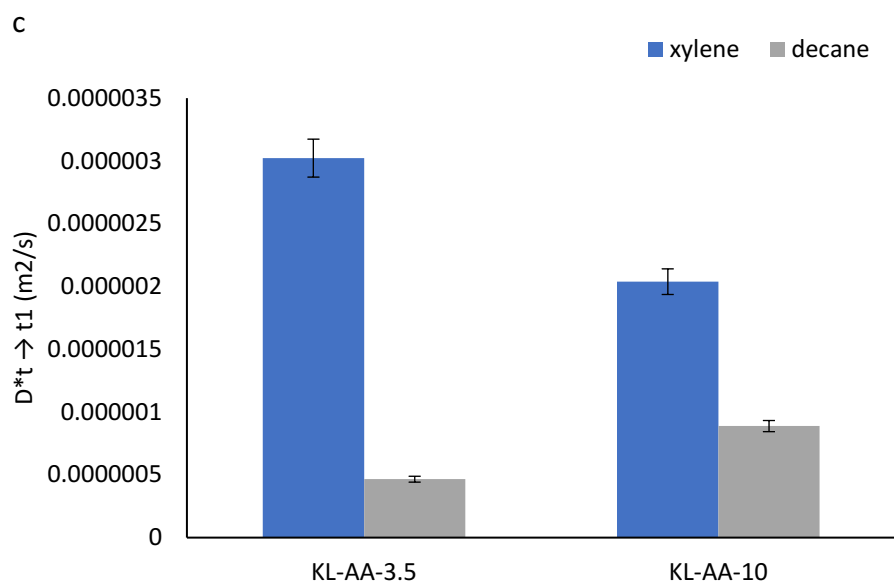
c

d
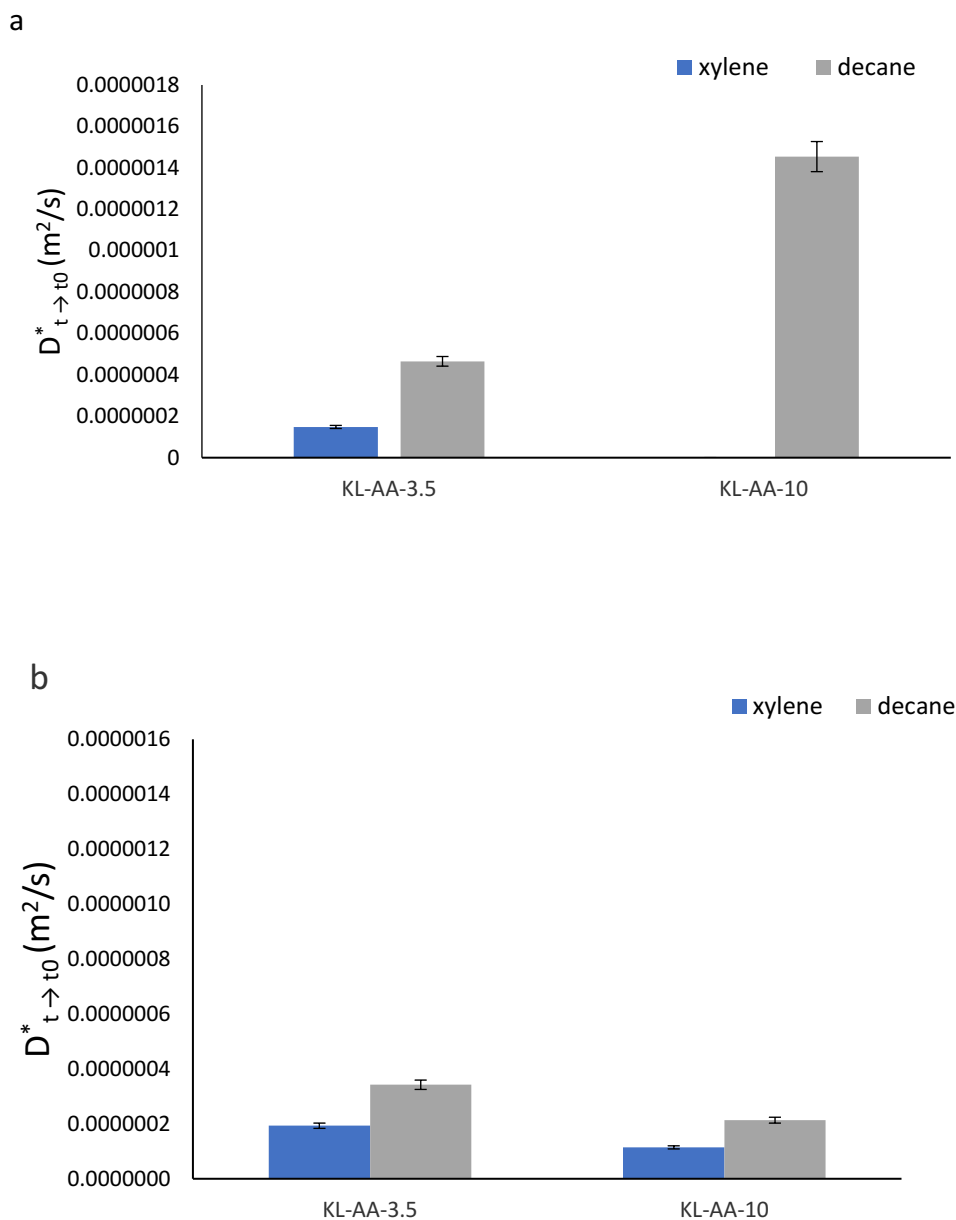
Figure 4.7. Diffusion coefficients at stage 1 for a) 1 wt.%, b) 2 wt.% and at stage 2 for 1 wt.% and 2 wt.% of KL-AA-3.5 and KL-AA-10 into oil-water emulsions

4.7. Contact angle measurements

Two-phase (water contact angle WCA), and three-phase contact angle (oil contact angle OCA) of a solid interface KL-AA at an air-water and oil-water surface were measured accordingly (Hu and Russell 2021). The adsorption of KL-AA on the surface will occur when the equilibrium of the three-phase contact angle, θ, exists (Garbin et al. 2012).

Figures 4.8 and 4.9 display the water contact angle (WCA) and three-phase contact angles (OCA) of 3 samples (pristine, KL, and KL-AA-10). The results show that the WCA and OCA contact angles significantly were affected by different solvents. Previously, the contact angle of water was 46.33˚ (Figure 4.8). With adding KL, the contact angle decreased to 35˚. Interestingly, KL-AA-10 dropped the contact angle even further, which is related to the more carboxylic acid group, molecular weight, and solubility of KL-AA. Also, the larger contact angle for cyclohexane and decane than xylene interfaces (i.e., larger OCA˚) is aligned with the larger contact angle of pristine oil-water emulsion. As seen, the changes for the OCA of decane-containing samples were larger than other samples (42˚, 40˚, and 20˚), implying the better compatibility with the oil interface. The results should be associated with the limited electrostatic that would control the stability of the emulsions (Fritz et al. 2017; Qiu et al. 2020).
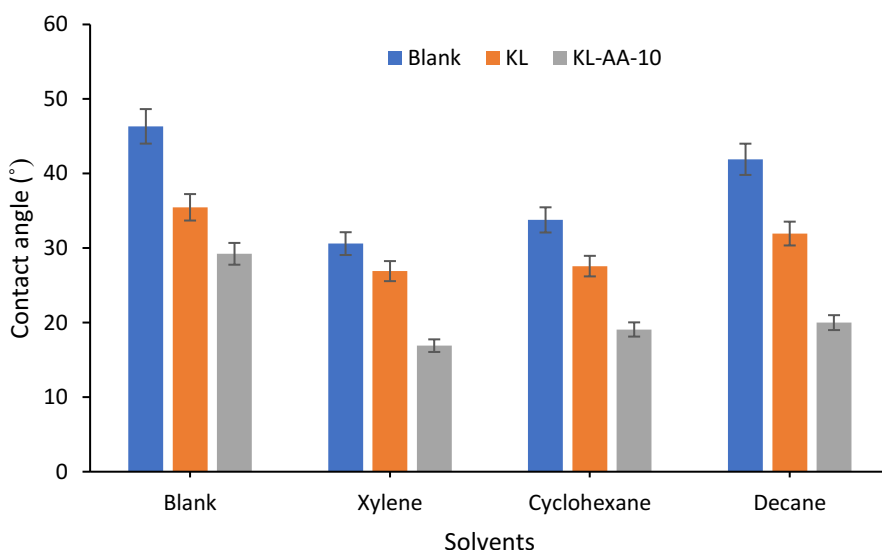

Figure 4.8. Contact angle of pristine and KL-AA containing oil-water emulsions
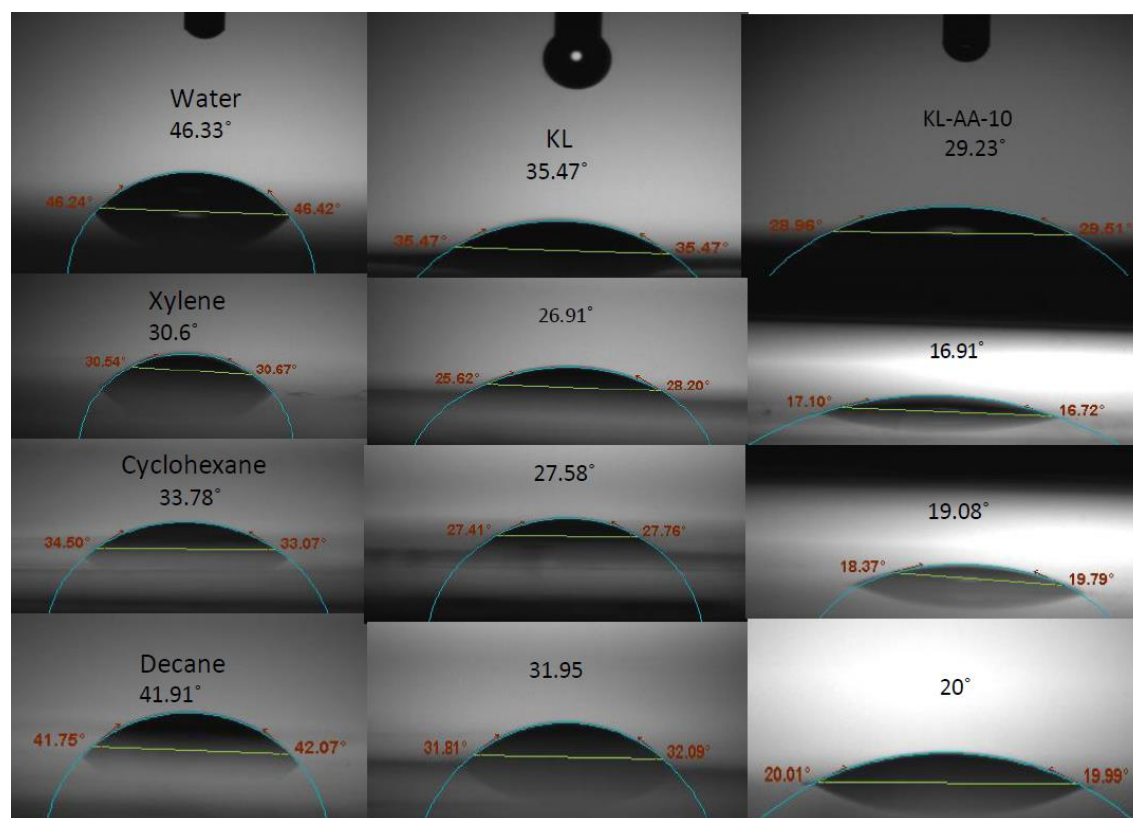
Figure 4.9. WCA and OCA of water, KL, and KL-AA-10

4.8. Adsorption of lignin-acrylic acid on oil

Three coated sensors of Al_2O_3 with xylene, cyclohexane, and decane were used for the adsorption experiment of KL-AA-3.5 and KL-AA-10. The deposition of KL-AA-3.5 and KL-AA-10 on coated sensors would change the frequency and dissipation of sensors. Figure 4.10 shows the frequency (Δf) and the dissipation (ΔD) changes of the coated sensors as lignin derivatives were deposited on them. The KL-AA samples were injected after buffer rinsing. It is seen that the frequency was generally decreased while dissipation was increased when KL-AA was deposited on the coated sensors. After buffer sensing, the frequency and dissipation changes were reduced. For xylene coated sensor, KL-AA-10 made overall larger frequency and dissipation changes. In all cases, however, a smaller $\Delta D/\Delta f$ was observed for KL-AA-3.5 without a significant dissipation change verifying a fairly inflexible characteristic of the adsorbed layer on the coated sensor (Sabaghi and Fatehi 2021). On the other hand, KL-AA-10 created a more viscoelastic adlayer on the coated sensors. Figure 4.11 shows the adsorbed mass and thickness of KL-AA on the coated

sensors. It is seen that KL-AA-10 deposited more and created thicker adlayer than KL-AA-3.5 on xylene coated sensor, which is in opposition to the adsorption on the other sensors. These results confirm that the KL-AA with more charges (KL-AA-10) interacted with the polar oil more than other oils. These results suggest that KL-AA-10 created more tail and loop configuration on the xylene sensor and probably entrapped more water within its adsorbed adlayer structure (Sabaghi et al. 2021). Therefore, the deposition of KL-AA-10 induced the surface to be more hydrophilic as the contact angle results confirmed (Figure 4.9).
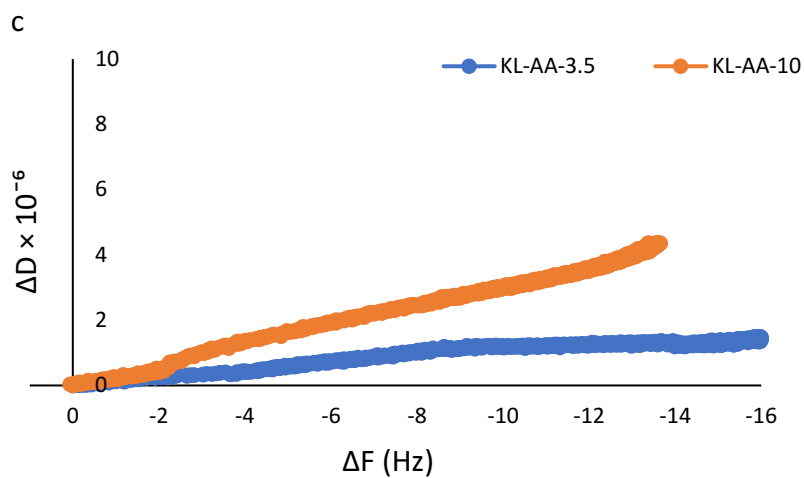
c
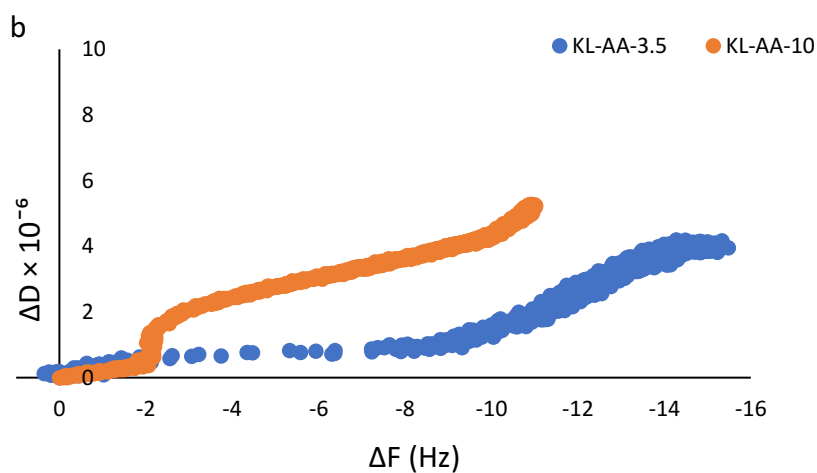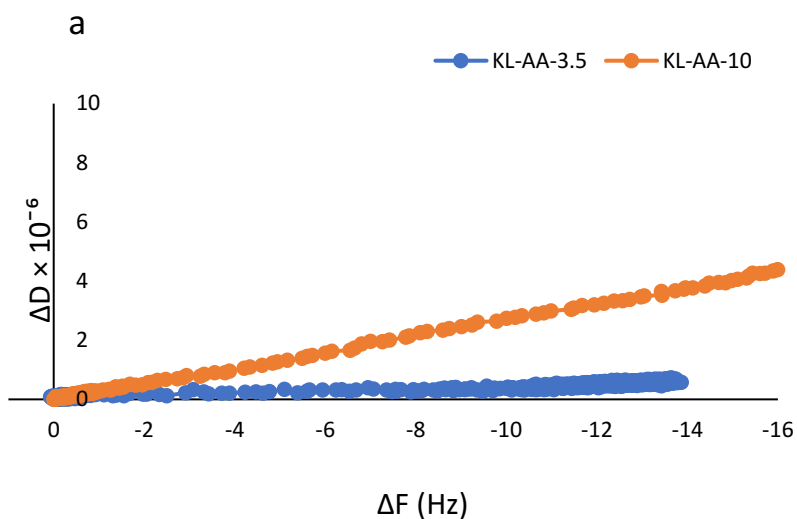
Figure 4.10. Dissipation changes of the sensors as a function of frequency changes upon adsorption of KL-AA polymers at a) xylene, b) cyclohexane and c) decane coated sensors

a

d

KL-AA-3.5   KL-AA-10

Thickness, nm

5
4
3
2
1
0

0   500   1000   1500   2000

Time, s

e

KL-AA-3.5   KL-AA-10

Thickness, nm

4
3
2
1
0

0   500   1000   1500   2000

Time, s
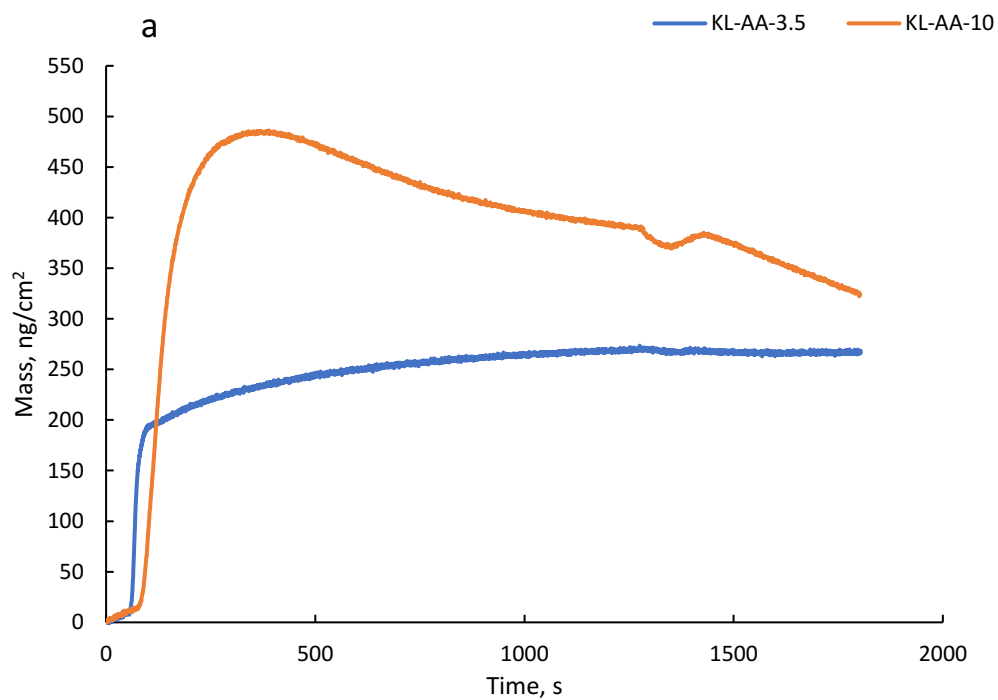
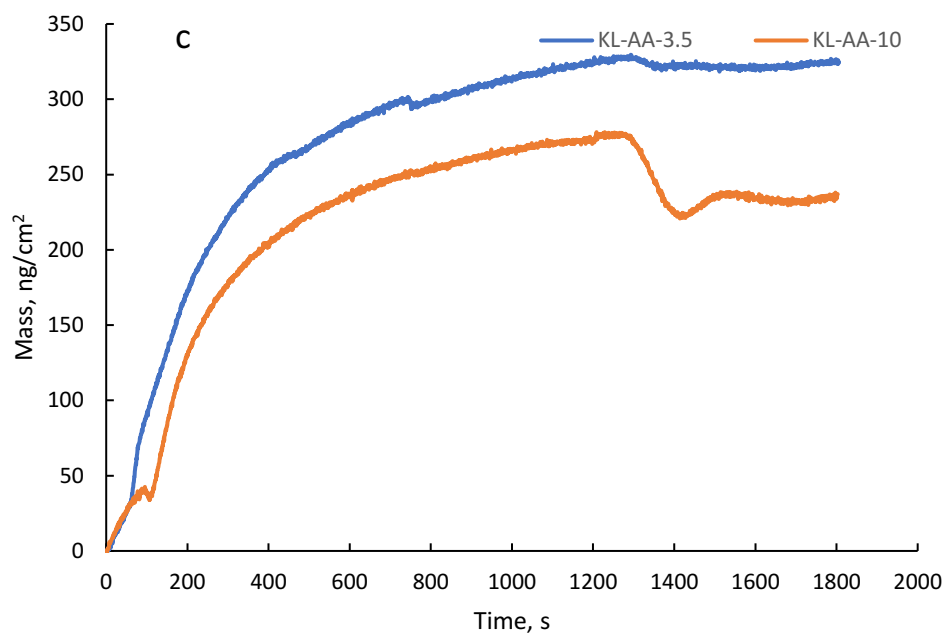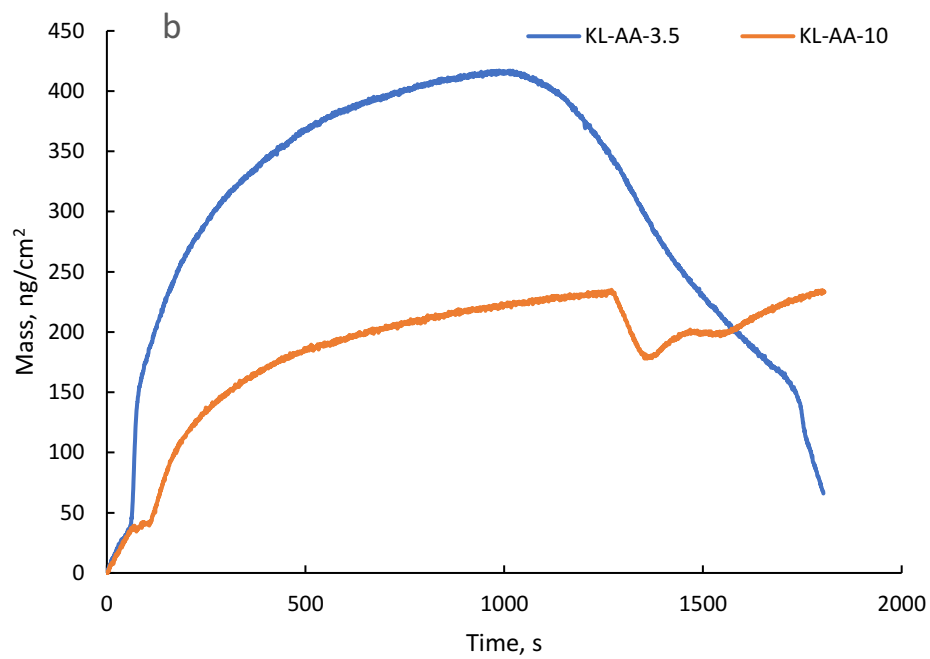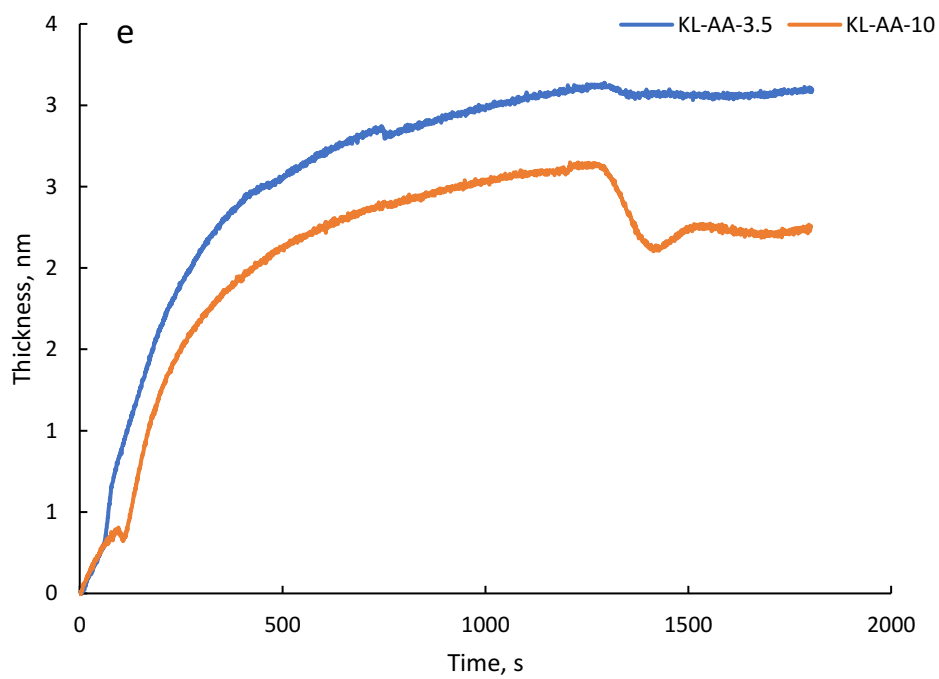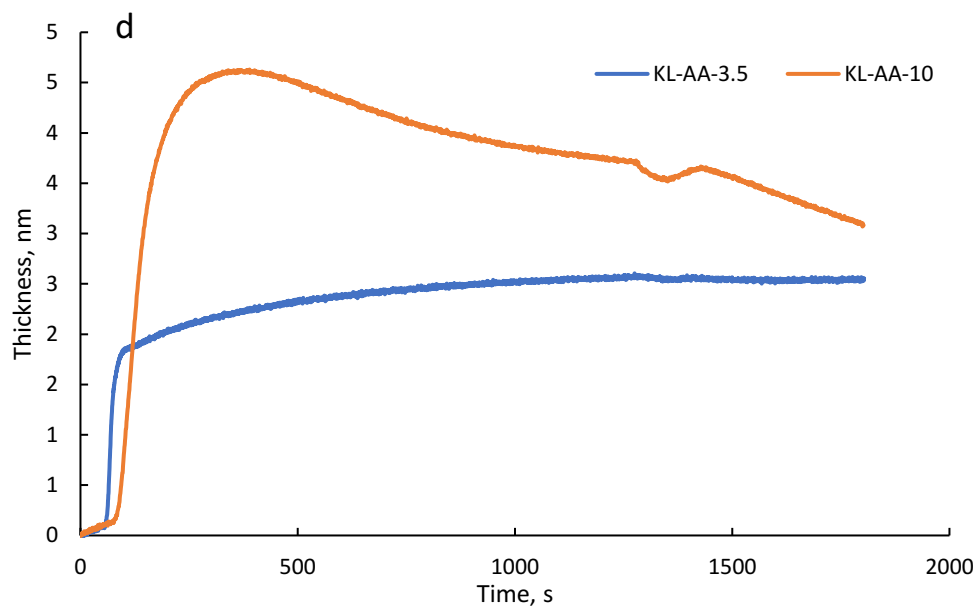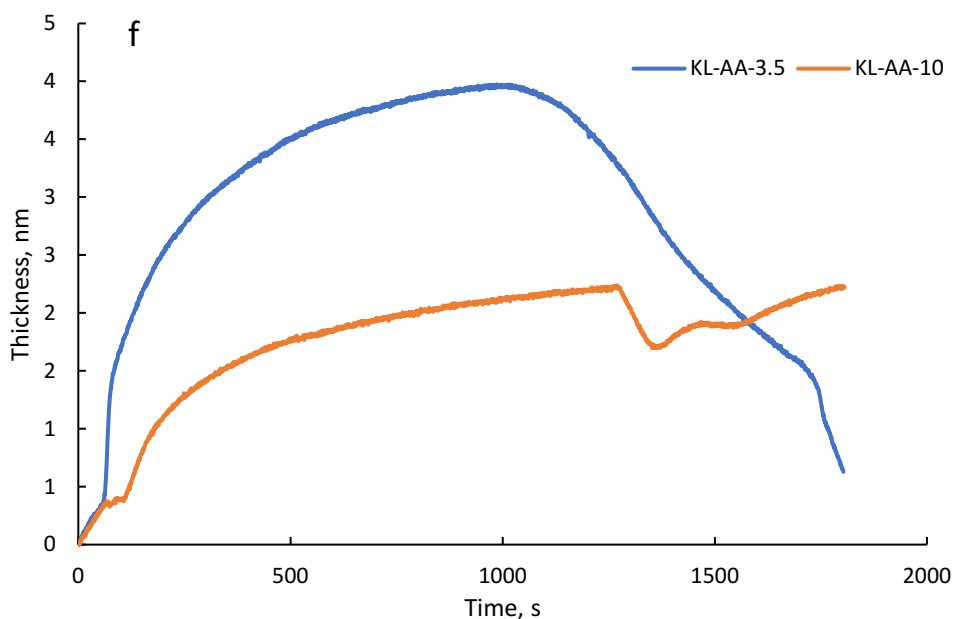Figure 4.11. Adsorbed mass of KL-AA polymers on a) xylene, b) cyclohexane and d) decane sensors, the thickness of the adsorbed mass on d) xylene, e) cyclohexane and f) decane sensors

4.9. Rheology measurement

The rheological properties of oil-water emulsions at different KL-AA concentrations were monitored by measuring their viscosity as a function of shear rates (Figure 4.12). It is observable that all emulsions follow non-Newtonian behavior. The viscosity and thixotropy (time-dependent shear thinning behavior) of polymeric materials are related to their microstructure (Guion and Hood 2016). Evidently, there is a distinguishable viscosity difference among the emulsions (Figure 4.12). At shear rate of 0.1 1/s, the viscosity of emulsions were 0.22, 0.29 and 0.31 Pa.s at 1wt.% KL-AA-3.5, KL-AA-7.5, and KL-AA-10, respectively. However, with increasing the concentration of KL-AA-3.5, KL-AA-7.5, and KL-AA-10 to 2 wt.%, the emulsions had more shear-thinning behavior with the viscosity of 0.48, 0.92, and 1.11 Pa.s, respectively. It has been reported that the changes in emulsion viscosity are generally affected by the interactions between the molecules/particles in the continuous phase and at the surfaces of the oil droplets (CA et al. 2012). Generally, a decrease in the viscosity of samples (Figure 4.12) is related to the continuous separation of phases as oil dropped accumulated on top of the system (Gharehkhani et al. 2018). The

stress applied to the droplets results in the division of droplets. If the stress is smaller than interaction forces between droplets, the emulsion will present elastic behavior and the energy will be stored as the distribution of the bonds between the dispersed droplets (Torres et al. 2007). In the same context, Li et al. (2016) suggested that the ion-dipole attraction between carboxymethylated lignin (CML) molecules and kerosene oil droplets elevated the fluid viscosity. As seen, KL-AA-10 generated a higher viscosity for all samples, as it had a larger molecular weight and charge density (Table 4.1). Based on Stokes' equation (Allen et al. 2016), it is known that creaming is accelerated by large droplet size and low viscosity of the continuous phase (Zhao et al. 2018).

In the xylene-water system (Figure 4.12), the enhanced viscosity of the system in the presence of KL-AA-10 slowed the droplet migration rate and the number of collisions between oil droplets stabilizing the emulsion. Therefore, the higher viscosity along with smaller droplet size improved the emulsion stability for the sample containing KL-AA-10. A similar phenomenon was observed for the cyclohexane-water system at 1 and 2 wt.% KL-AA concentration (Figure 4.12) and for the decane-water system at 1 wt.% KL-AA concentration (Figure 4.12). In the case of the decane-water system at 2 wt.% KL-AA, the viscosity of sample containing KL-AA-10 was slightly lower than other decane-water systems at a low shear rate, but it was higher than other decane-water systems at a high shear rate. Also, at 2 wt.% concentration, the viscosity of all samples was higher than that at 1 wt.% concentration, which is attributed to the addition of KL-AA that inhibited the movement of droplets and thus stabilized the systems. Also, as KL-AA would generate self-aggregate at 2 wt.% concentration, the particles of KL-AA derivatives in the emulsions probably helped with the viscosity variations.
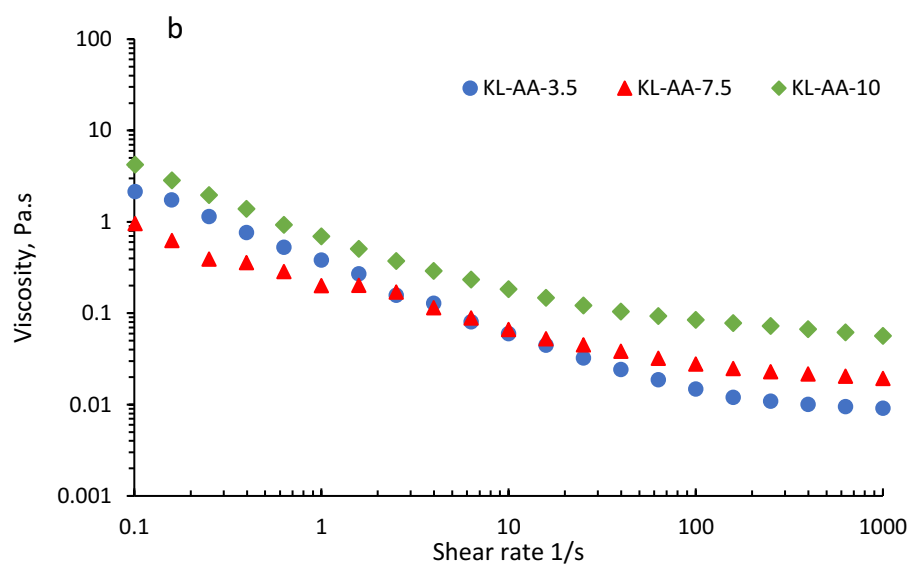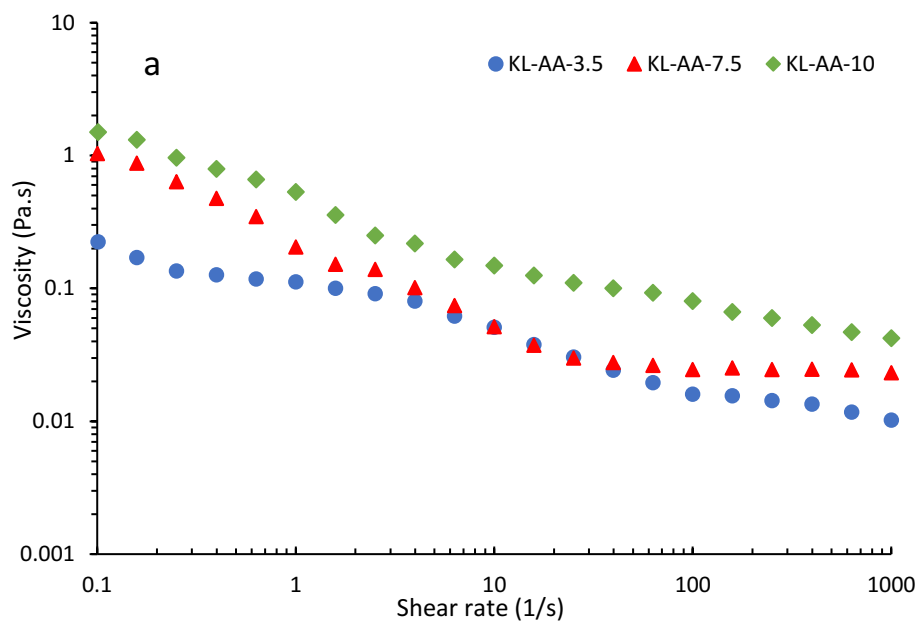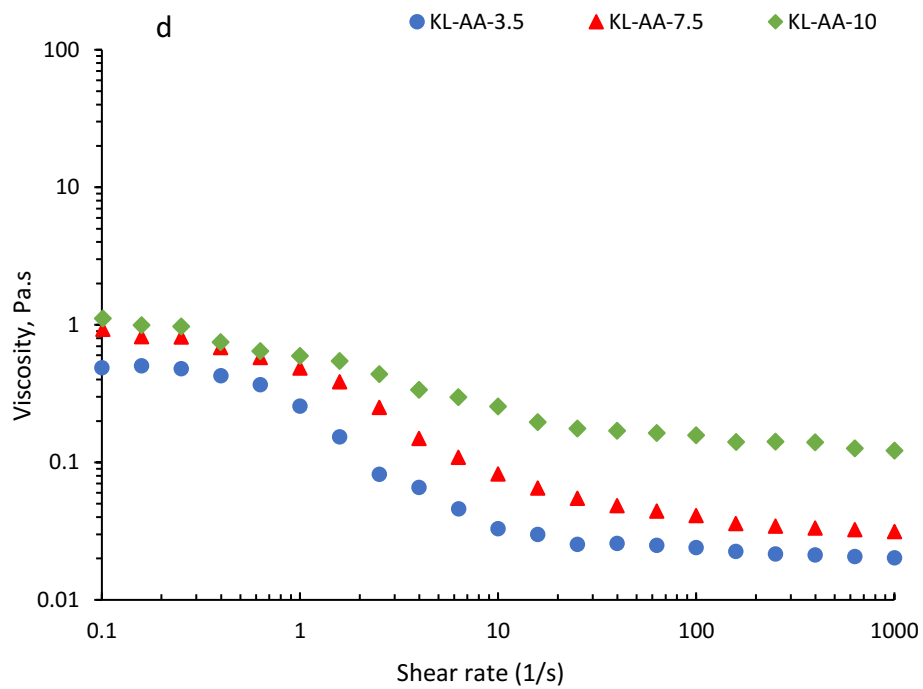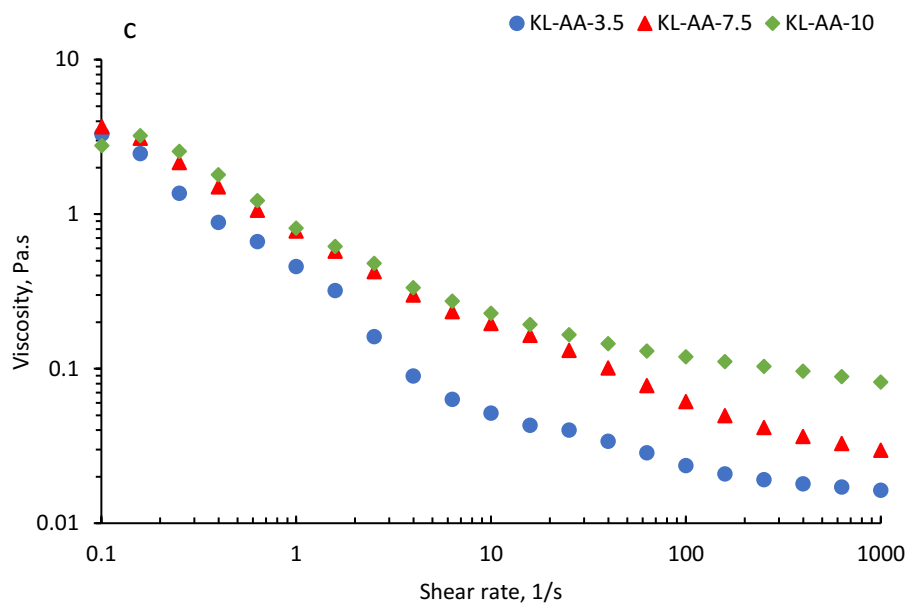
Figure 4.12. Viscosity of KL-AA polymers at a 1 wt.% concentration of a) xylene, b) cyclohexane, c) decane, and 2 wt.% concentration of d) xylene, e) cyclohexane and f) decane
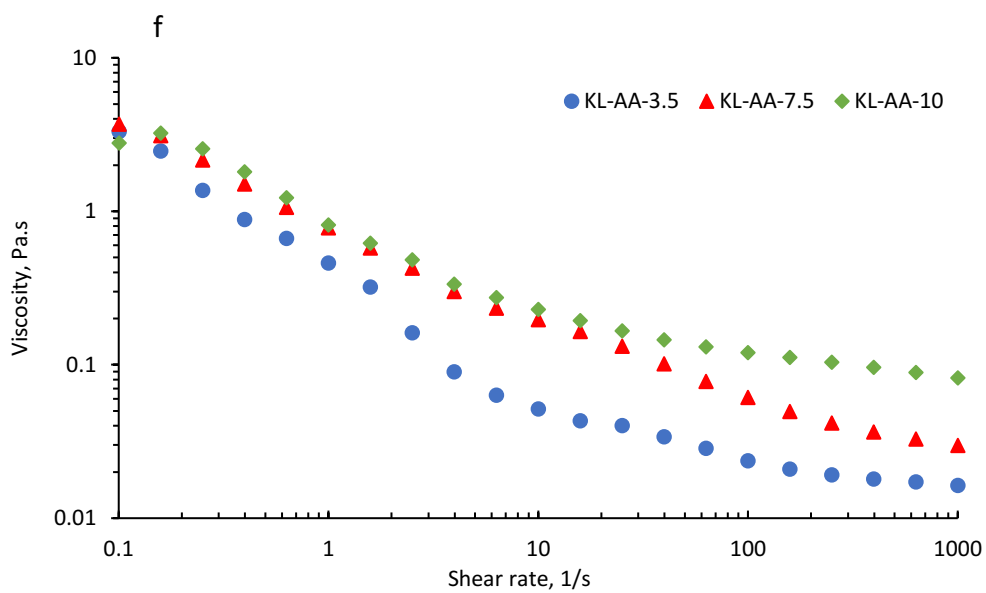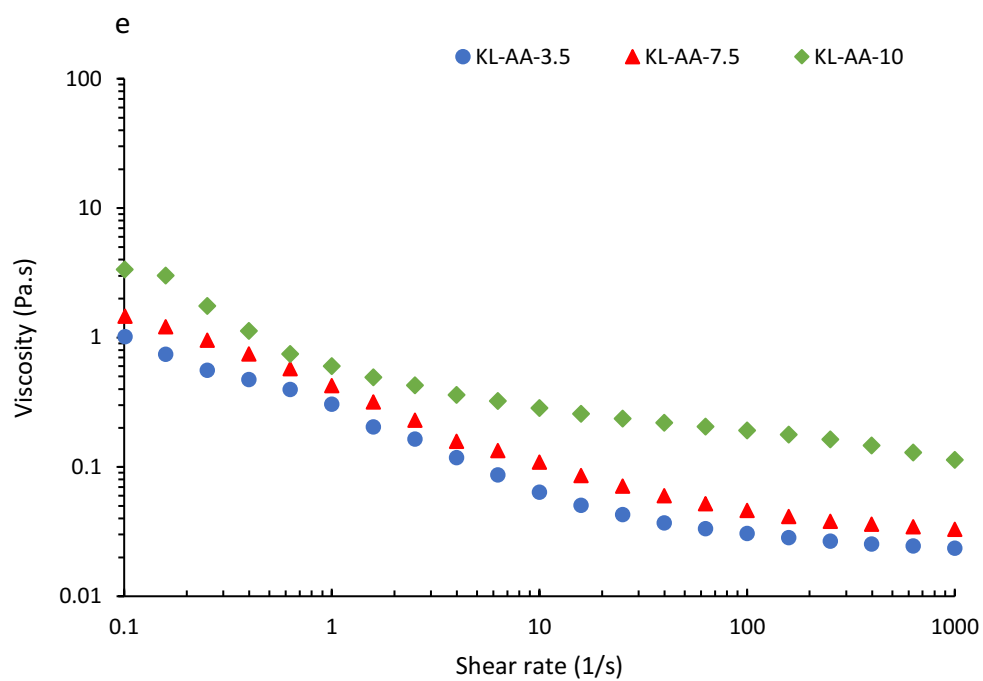
In Figure 4.13, the impact of solvents on the rheological properties is shown. The emulsion containing decane and KL-AA at 1 wt.% concentration had higher viscosity as KL-AA could interact with decane and promote its decane droplet formation (Ghavidel and Fatehi 2021). Generally, dynamic shear tests often refer to oscillatory amplitude sweeps under a constant angular frequency in rheology investigation. It was suggested that the yield stress (or strain) can be determined from the crossover point of apparent elastic moduli G′ and viscous moduli G″ by plotting them against either the shear stress or strain amplitude (Yang et al. 2017). One of the methods to understand the elastic behavior of a system is to determine its yield point. For instance, (Walls et al. 2011) reported that the maximum elastic stress curve is the yield stress when the elastic stress ($G'\gamma_0$ with γ_0 the strain amplitude) is plotted versus strain amplitude. Heymann et al. (2002) followed the same concept in the transient shear ramp tests and illustrated that the plot of shear stress amplitude versus shear strain amplitude was nearly independent of the frequency below the apparent yield stress, while the plot of shear stress amplitude versus shear rate amplitude shows a Newtonian flow range above the critical shear stress amplitudes.
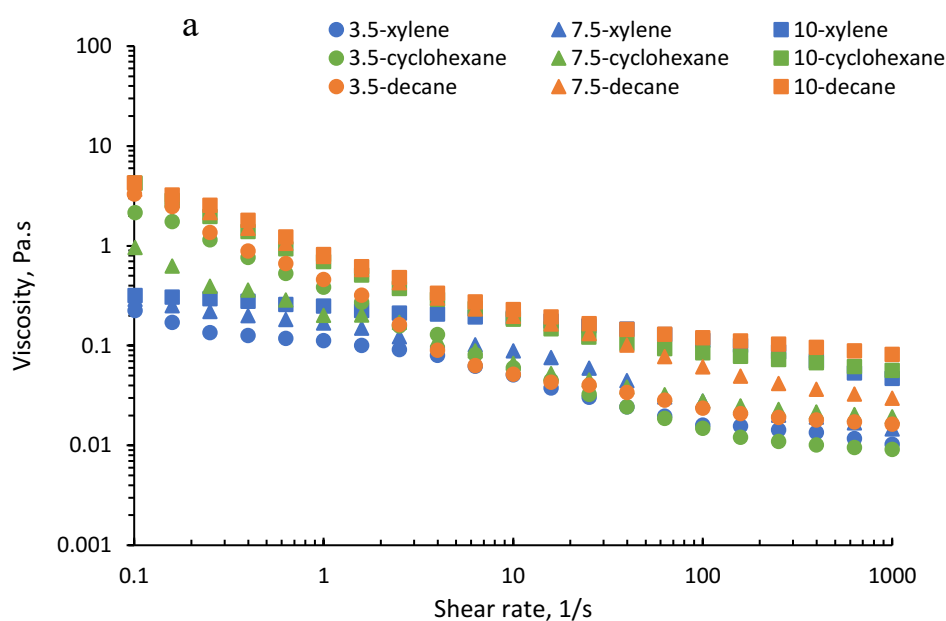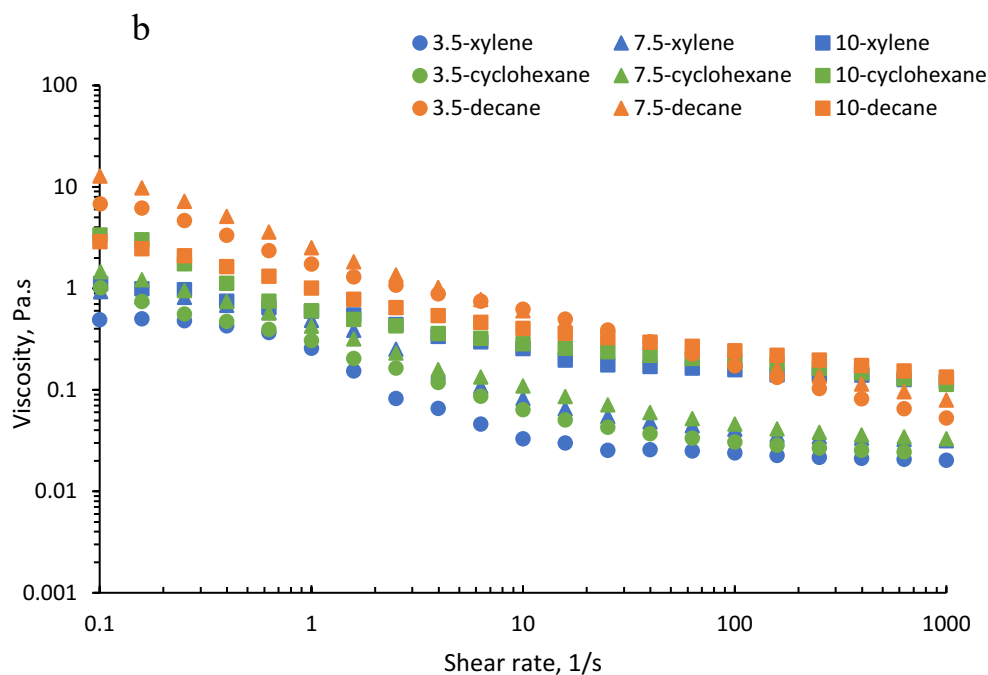
Figure 4.13. Viscosity versus the shear rate of KL-AA polymers, a) at 1 wt.% and b) at 2 wt.% concentration

To understand the behavior of the emulsion, we investigated the stress and strain amplitudes of the samples, and Figure (4.14) shows measured G′ and G″ of the emulsion systems as functions of stress or strain amplitudes (Yang et al. 2017). At 1 wt.% concentration, the apparent G′ and G″ are almost independent of stress (or strain) amplitudes and G′ are larger than G″ at very low stress (at rest) amplitudes range, which implies linear viscoelastic behavior and elastic domination (Yang et al. 2017). All of the emulsions have viscoelastic behavior at 1 wt.% concentration for xylene-water emulsions. However, they had liquid-like behavior at 2 wt.% concentration. When the deformation is sufficiently large to break the structure and initiate the flow of the system, the apparent G′ decreases, and G″, the viscous subscription, dominates the elastic subscription.

In the same vein, the oscillation amplitude results for cyclohexane show that by increasing the strain (%) from 0.1 % shear strain to 100%, the sample lost its elasticity and behaved like a liquid. In the case of the decane sample (Figure 4.14), at low concentration (1 wt.%), emulsions have elastic behavior at 0.1% shear strain; and by increasing the strain to 100 (%), the behavior of the emulsion was changed from elastic to liquid-like at both 1 and 2 wt.% (Figure 4.14). The elastic

modulus of the lignin systems may be associated with the presence of very strong hydrophobic forces among the emulsifier molecules (Magual et al. 2005). Higher lignin concentration encourages an increase in the self-aggregation and self-organization of KL-AA at the interface (Figure 4.3), thus reducing their impact on the viscoelastic behavior of the samples (Shulga et al. 2011).

d

e
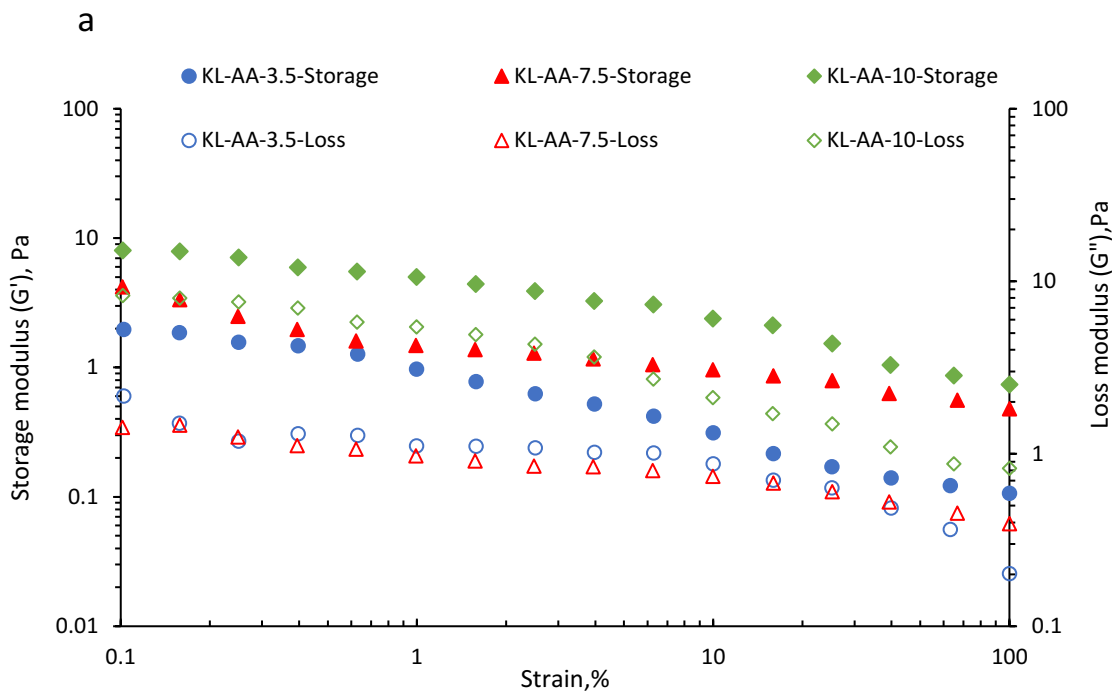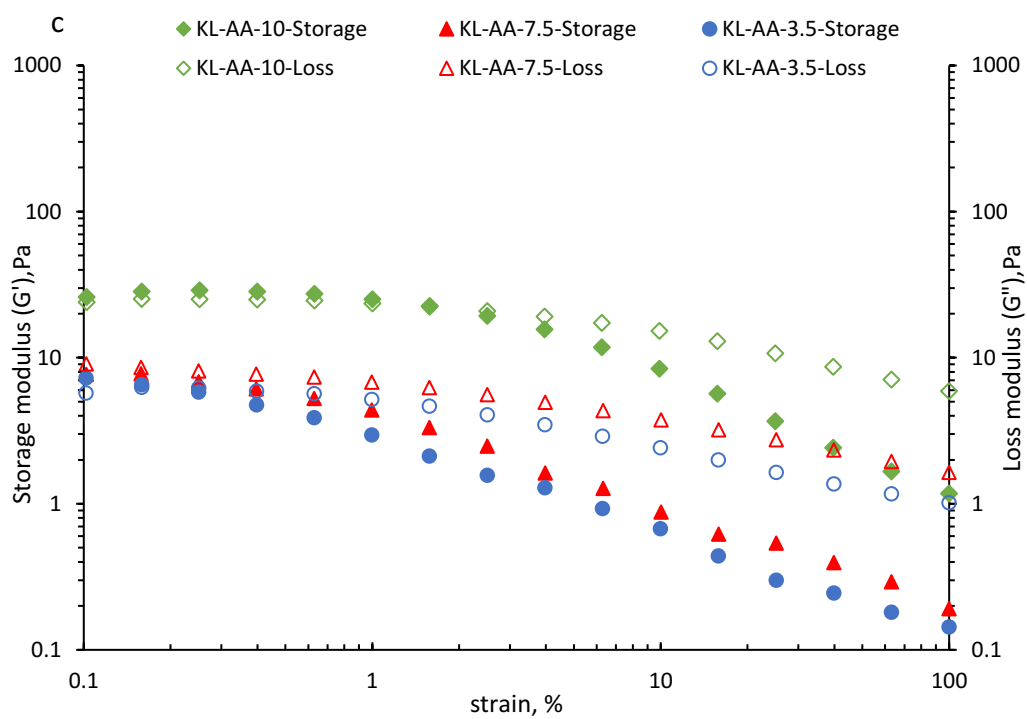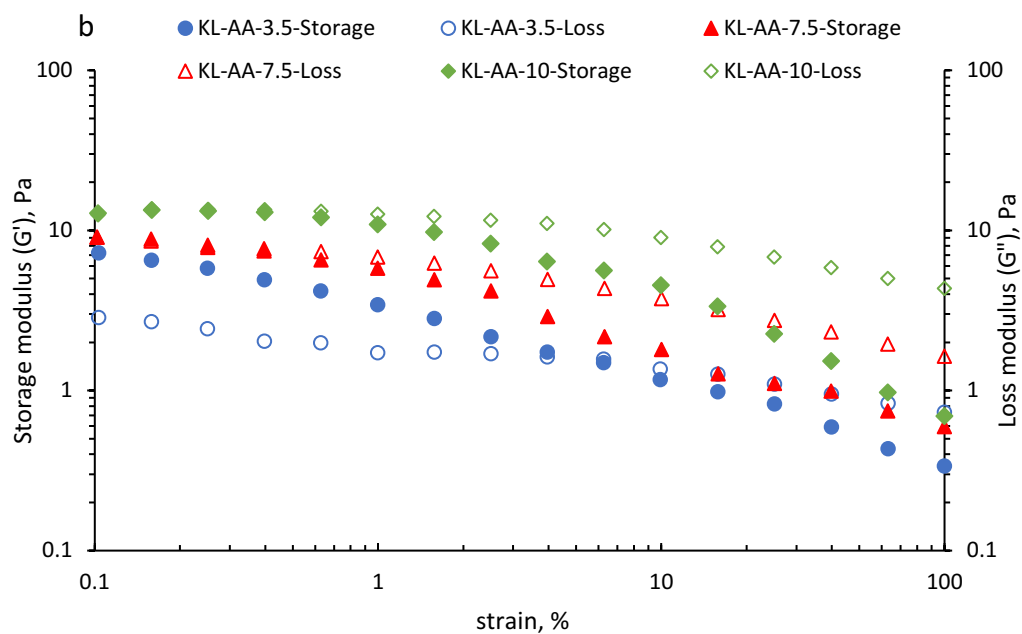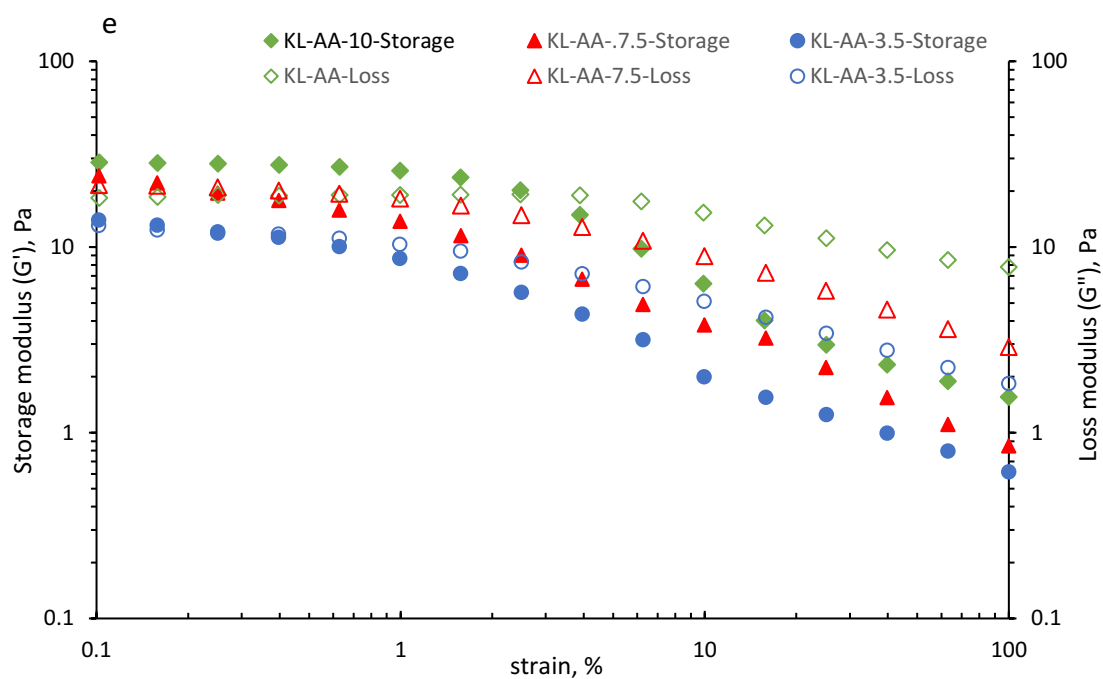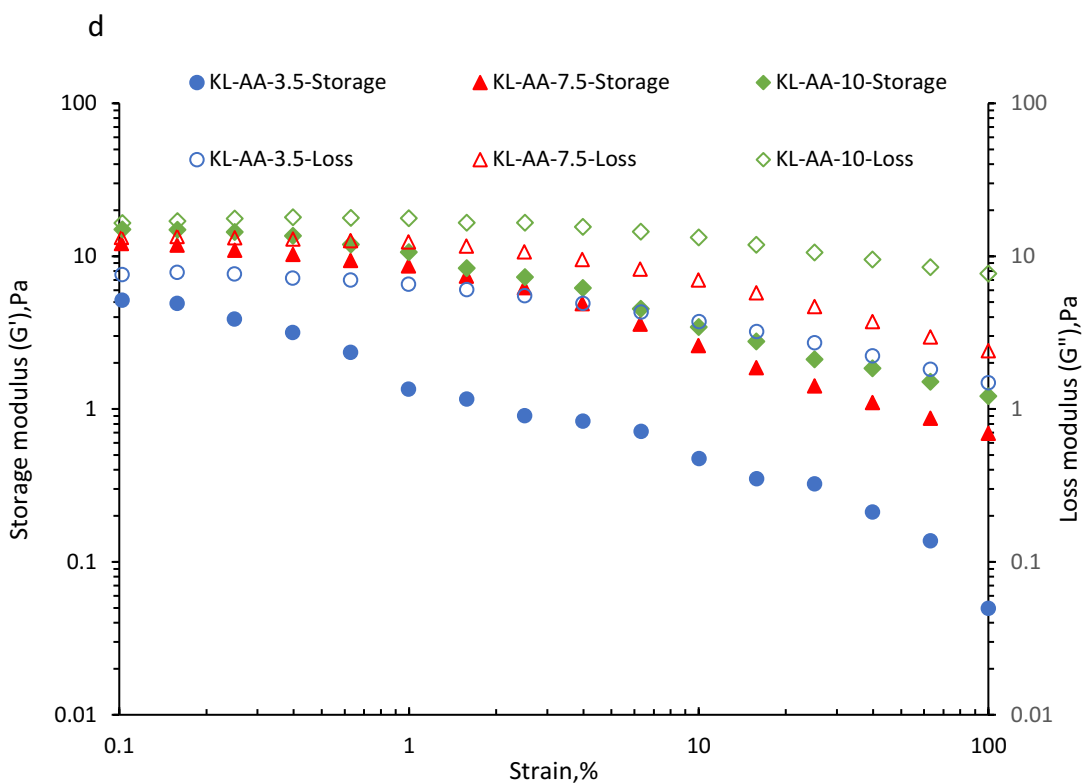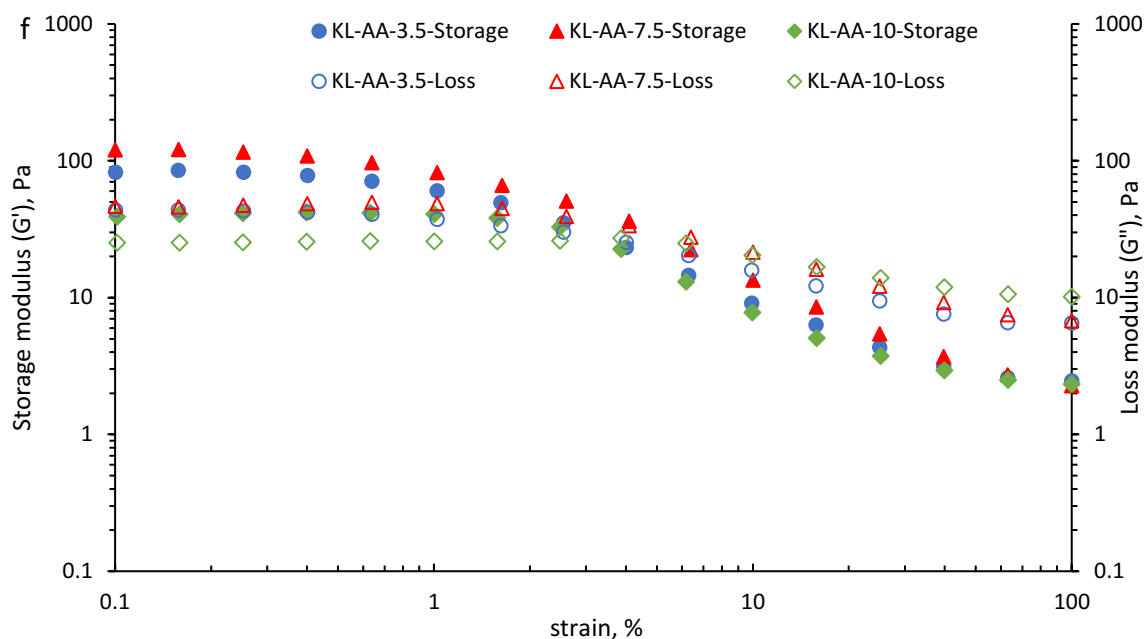
Figure 4.14. G′ and G″ versus strain (%) of xylene, cyclohexane and decane solvents at 1 wt.% concentration of a) xylene, b) cyclohexane, c) decane, and 2 wt.% concentration of d) xylene, e) cyclohexane and f) decane

4.10. Confocal visualization

Figure 4.15 shows the confocal images of the emulsions formulated from different oils. The oil phase is demonstrated by green color as was marked by the dye. The variations in the oil droplet size are observable by changing the oil type and KL-AA polymers. It is inferred that xylene, as the oil phase, contributed to the formation of the largest oil droplets, while decane displayed the smallest droplet size at 2 wt.% KL-AA concentrations. The findings follow previous observations reported on the formulation of larger oil droplets for polar oils compared to non-polar oils (Bai et al. 2019). Also, a possible explanation might be the higher interfacial adsorption of KL-AA at the decane interface (Figure 4.10), which facilitated the production of small droplets. As it is also seen in KL-AA-10 generated smaller drop particles than other KL-AA derivatives, which is attributed to the higher adsorption of this polymer at the interface, as stated earlier (Figure 4.10).
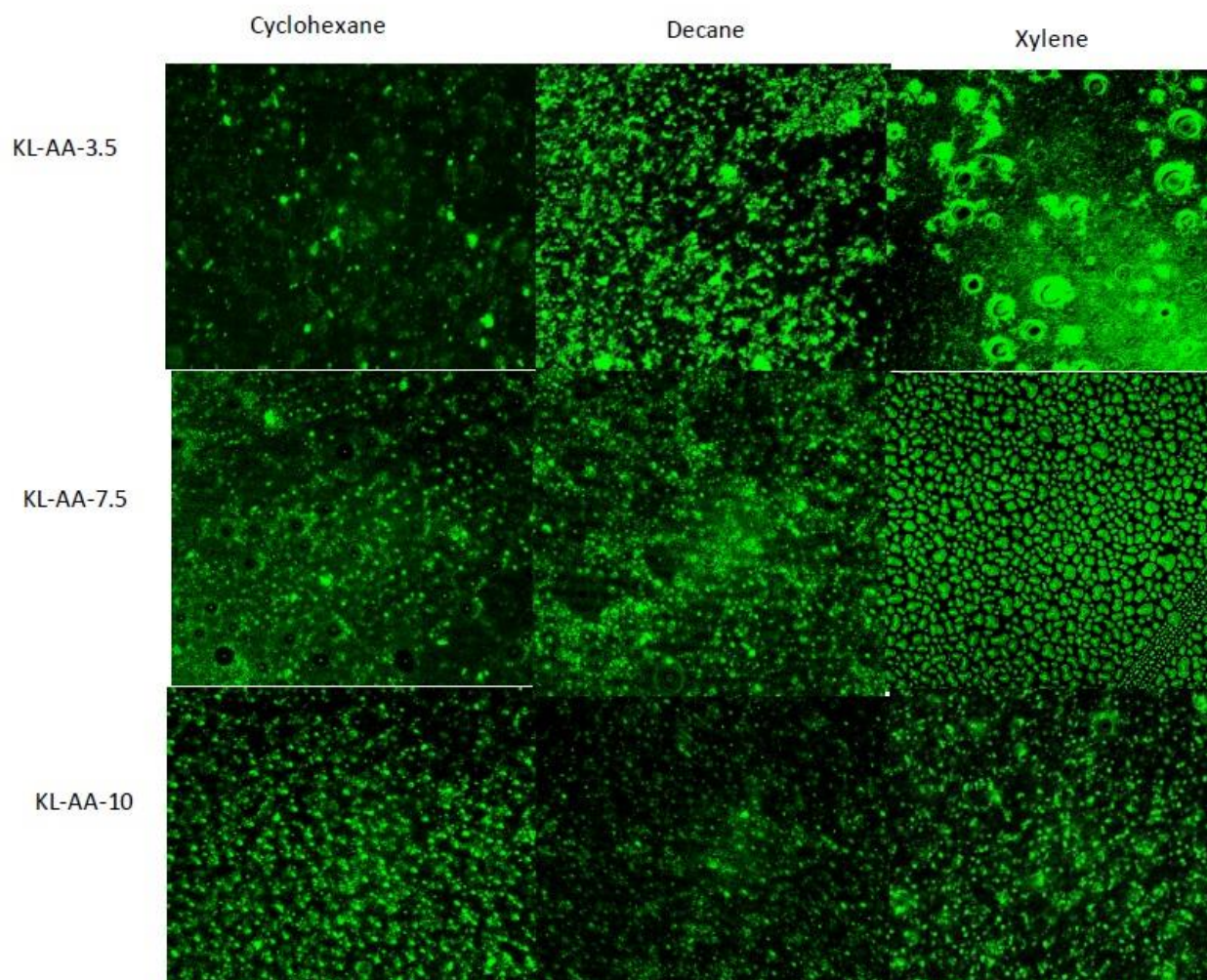
Figure 4.15. Confocal images of the emulsions prepared from xylene, cyclohexane, and decane as the oil phase and KL-AA derivatives at 2 wt.% concentration

4.11. Stability assessment

The 24-h stability of three samples (KL-AA-3.5, KL-AA-7.5, and KL-AA-10) with three solvents (xylene, cyclohexane, and decane) at 1 and 2 wt.% concentrations was examined with a stability analyzer and the results are shown in Figure 4.16. KL-AA-10 showed more stability and lower sedimentation rate compared to other KL-AA polymers, as it has more charges, carboxylic group, and molecular weight intensifying the repulsion between KL-AA-10 molecules adsorbed on oil droplets and thus they could limit the interactions of oil droplets. As also seen, decane samples were more stable than other emulsions, which was also observed in the results observed in the

rheology analysis (Figure 4.12 to 4.14). Such results are attributed to the lower polarity of decane than other oils (i.e., close to that of water) (Ghavidel and Fatehi 2021).

c

d
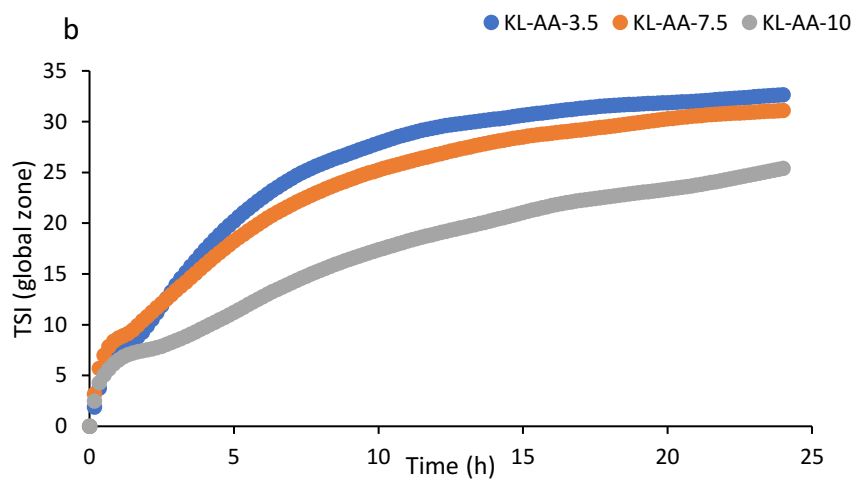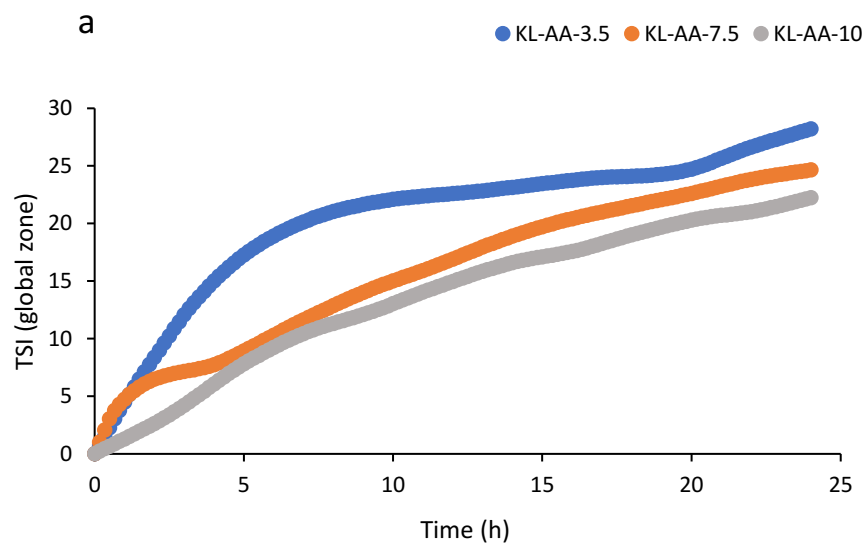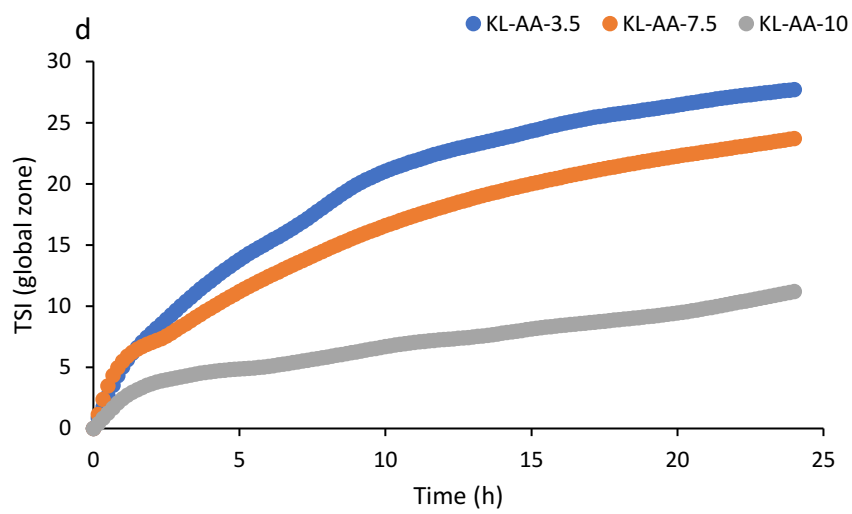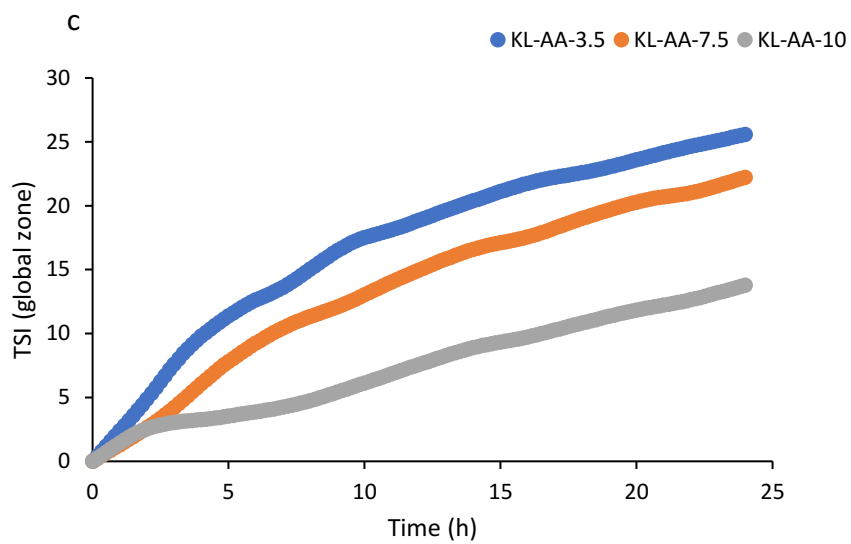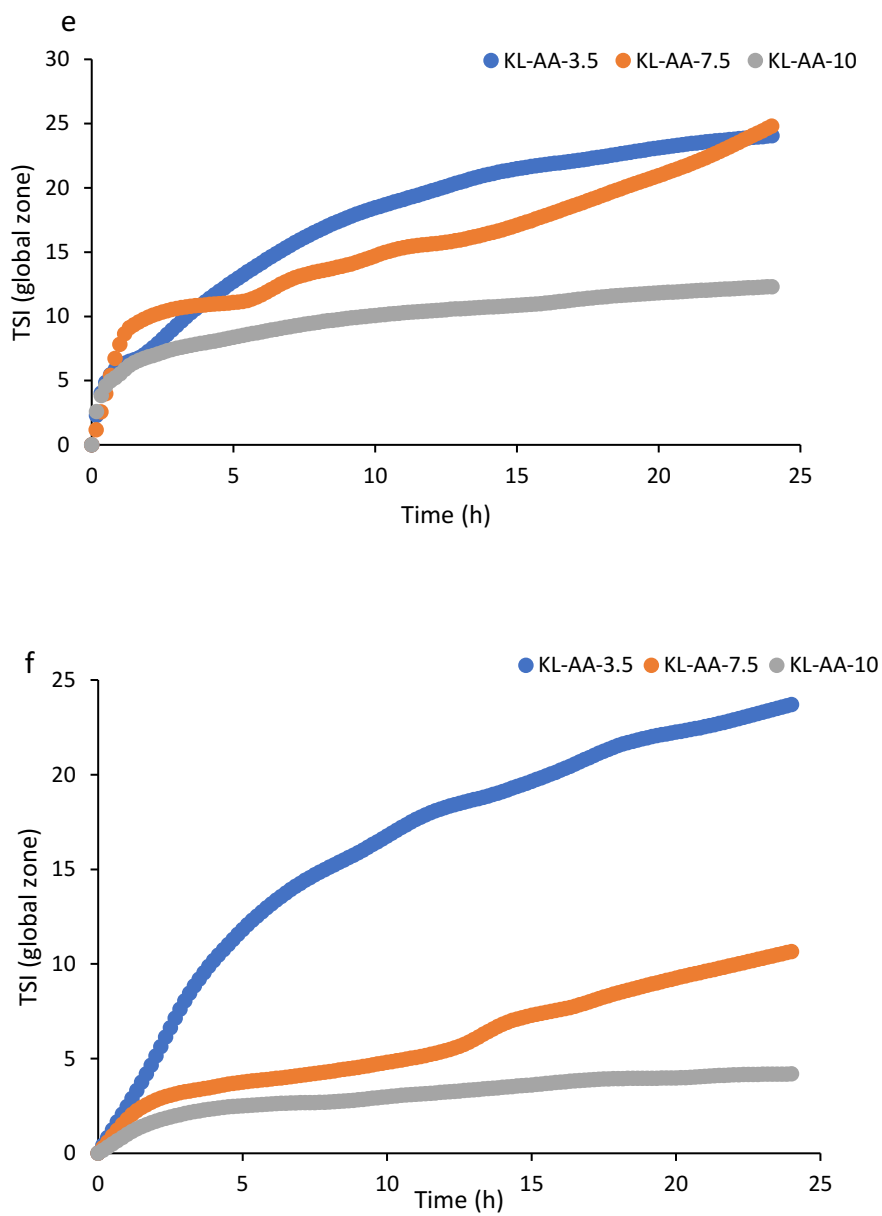
Figure 4.16. The TSI value of oil/water emulsion of xylene, cyclohexane, and decane in the presence of KL derivatives at 1 wt.% concentration of a) xylene, b) cyclohexane, c) decane, and 2 wt.% concentration of d) xylene, e) cyclohexane and f) decane

Chapter 5. Conclusions and Recommendations

5.1. Conclusions

In this thesis, lignin-acrylic acid polymers (KL-AA) with different molecular weights, charge densities, and carboxylic acid groups were generated, and their properties were comprehensively verified. The critical aggregation concentrations of KL-AA were 1.5 wt.%, and thus two different concentrations of 1 and 2 wt.% were chosen in this analysis. The KL-AA-10 with the highest carboxylic acid group varied the zeta potential of water the most, which is attributed to its highest charge density.

It was observed that KL-AA-10 dropped the surface tension of water the most and dropped the water contact angle and oil contact angle of the oil-water system the most. These results imply that the higher charge of the KL-AA polymer promoted the interaction of water and oil. Also, the emulsion containing KL-AA-10 had the highest viscosity and stability and smallest droplet size among emulsions containing other lignin derivatives. However, the lignin derivative with the lowest carboxylic acid group, KL-AA-3.5, adsorbed more than other lignin derivatives on the surface of oils as it was smaller and induced a smaller repulsion force for other KL-AA-3.5 to adsorb on the surface.

Generally, better results were obtained for xylene water emulsion than other emulsions, regardless of lignin type, which is due to more polarity of xylene and thus better compatibility of xylene and water. However, the impact of lignin derivatives was more sensible for the decane water emulsion implying that more dramatic changes were observed for this emulsion when lignin derivatives were added to the decane-containing emulsion. These results are due to the fact that decane was the least polar oil among all, and the non-polarity of lignin helped facilitate the interaction and thus miscibility of decane and water.

It was also observed that the 2 wt.% of lignin derivatives induced more adsorption on the oil surface, which impacted the contact angle and interface tension of the emulsions more greatly and generated more stable emulsions. However, the presence of lignin aggregates at higher lignin concentrations did not improve the rheological properties of the emulsion.

Overall, it can be concluded that lignin acrylic acid can be an effective emulsifier for oil-water emulsions, and the properties of the polymer will impact its emulsifying performance. Although better results can be obtained for the oil-water mixtures that have two compatible phases, the impact of lignin acrylic acid on the emulsification of oil water mixture was more observable for the two more immiscible phases.

5.2. Recommendations

This thesis illustrated how lignin acrylic acid polymer can act as an emulsifier. Lignin can be decorated with various charged groups, e.g., aminated and sulfonated groups. It is suggested that the impact of these lignin derivatives be also assessed in emulsifying oil-water emulsions. Also, this work can be extended to include emulsions with other oil types to generate more comprehensive conclusions.

Nomenclature

Abbreviations

CAC	Critical aggregation concentration
KL-AA	Kraft lignin acrylic acid
KL-AA-3.5	Kraft lignin acrylic acid polymer with lowest carboxylic acid group
KL-AA-7.5	Kraft lignin acrylic acid polymer with medium carboxylic acid group
KL-AA-10	Kraft lignin acrylic acid polymer with the highest carboxylic acid group
PAA	Poly acrylic acid
TSI	Turbiscan Stability Index
WCA	Water contact angle
OCA	Oil contact angle

Notations

ΔD	Dissipation change
Δf	Frequency change

Greek symbols

ζ	Zeta potential
γ	Surface tension
G'	Elastic moduli
G''	Viscous moduli

Subscripts and Superscripts

$D^*_{t \to 0}$	Diffusion coefficient in the first stage of adsorption
$D^*_{t \to 1}$	Diffusion coefficient in the second stage of adsorption

Chapter 6. References

References

Alinezhad K., Hosseini M., Movagarnejad K., Salehi M., Experimental and Modeling Approach to Study Separation of Water in Crude Oil Emulsion under Non-Uniform Electrical Field, Korean Journal of Chemical Engineering, 2010, 27(1), 198–205.

Alwadani N., Ghavidel N., Fatehi P., Surface and Interface Characteristics of Hydrophobic Lignin Derivatives in Solvents and Films, Colloids and Surfaces, Physicochemical and Engineering Aspects, 2021, 609, 125656.

Azadfar M., Gao A., Bule M., Chen S., Structural Characterization of Lignin, A Potential Source of Antioxidants Guaiacol and 4-Vinylguaiacol, International Journal of Biological Macromolecules, 2015, 75, 58–66.

Azadi P., Oliver R., Farnood R., King D., Liquid Fuels, Hydrogen and Chemicals from Lignin, A Critical Review, Renewable and Sustainable Energy Reviews, 2013, 21, 506–23.

Bai L., Lv Sh., Xiang W., Huan S., McClements D., Rojas O., Oil-in-Water Pickering Emulsions via Microfluidization with Cellulose Nanocrystals, Formation and Stability, Food Hydrocolloids, 2019, 96, 699–708.

Bergfreund J., Sun Q., Fischer P., Bertsch P., Adsorption of Charged Anisotropic Nanoparticles at Oil-Water Interfaces, Nanoscale Advances, 2019, 1(11), 4308–12.

Bi J., Yang F., Harbottle D., Interfacial Layer Properties of a Polyaromatic Compound and Its Role in Stabilizing Water-in-Oil Emulsions, Langmuir, 2015, 31(38), 10382–91.

Binks P., Dong J., Rebolj N., Equilibrium Phase Behaviour and Emulsion Stability in Silicone Oil water AOT Mixtures, Physical Chemistry Chemical Physics, 1999, 1(9), 2335–44.

Bizmark N., Ioannidis M., Ethyl Cellulose Nanoparticles at the Alkane-Water Interface and the Making of Pickering Emulsions, Langmuir, the ACS journal of surfaces and colloids, 2017, 33(40), 10568–76.

Bonto M., Eftekhari A., Nick H., An Overview of the Oil-Brine Interfacial Behavior and a New Surface Complexation Model, Scientific Reports, 2019, 9(1), 1–16.

Chaochanchaikul K., Jayaraman K., Rosarpitak, V., Sombatsompop N., Influence of lignin content on photodegradation in wood/HDPE composites under UV weathering, Bioresources, 2012, 7(1), 38-55.

Chakar FS., and Ragauskas AJ., Review of Current and Future Softwood Kraft Lignin Process Chemistry, Industrial Crops and Products, 2004, 20(2), 131–41.

Chen J., Kazzaz A., AlipoorMazandarani N,. HosseinpoorFeizi Z., Production of Flocculants Adsorbents and Dispersants from Lignin, Molecules 2018, 23(4), 868.

Costa C., Medronho B., Filipe A., Mira I., Lindman B., Edlund H., Norgren M., Emulsion Formation and Stabilization by Biomolecules, The Leading Role of Cellulose, Polymers, 2019, 11(10), 1570.

Czaikoski A.,Gomes A., Kaufman K., Liszbinski R., Jesus M., Cunha R., Lignin Derivatives Stabilizing Oil-in-Water Emulsions, Technological Aspects, Interfacial Rheology and Cytotoxicity, Industrial Crops and Products, 2020, 154, 112762.

Doherty W., Mousavioun P., Fellows C., Value-Adding to Cellulosic Ethanol, Lignin Polymers, Industrial Crops and Products, 2011, 33(2), 259–76.

Fainerman V., Aksenenko E., Miller R., Dynamics of Surfactant Adsorption from Solution Considering Aggregation within the Adsorption Layer, Journal of Physical Chemistry B, 1998, 102(31), 6025–28.

Fainerman, V., Makievski A., Miller R., The Analysis of Dynamic Surface Tension of Sodium Alkyl Sulphate Solutions, Based on Asymptotic Equations of Adsorption Kinetic Theory, Colloids and Surfaces, A Physicochemical and Engineering Aspects, 1994, 87(1), 61–75.

Fernandes M., Pires R., Mano J., Reis R., Bionanocomposites from Lignocellulosic Resources, Properties, Applications and Future Trends for Their Use in the Biomedical Field, Progress in Polymer Science, 2013, 38(10–11), 1415–41.

Figueiredo P., Lintinen K., Hirvonen J., Kostiainen M., Santos H., Properties and Chemical Modifications of Lignin, Towards Lignin-Based Nanomaterials for Biomedical Applications, Progress in Materials Science, 2018, 93, 233–69.

Fingas M., Fieldhouse B., Formation of Water-in-Oil Emulsions and Application to Oil Spill Modelling, Journal of hazardous materials, 2004, 107(1–2) 37–50.

Fritz C., Salas C., Jameel H., Rojas O., Self-Association and Aggregation of Kraft Lignins via Electrolyte and Nonionic Surfactant Regulation, Stabilization of Lignin Particles and Effects on Filtration, Nordic Pulp and Paper Research Journal, 2017, 32(4), 572–85.

Gao W, Alkhalifa Z, Fatehi P., Generation of Sulfonated Kraft Lignin Acrylic Acid Polymer and Its Use as a Flocculant, Separation Science and Technology, 2021, 56(9), 1601–1611.

Garbin V., Crocker J., Stebe K., Nanoparticles at Fluid Interfaces: Exploiting Capping Ligands to Control Adsorption, Stability and Dynamics, Journal of Colloid and Interface Science, 2012, 387(1), 1–11.

Gellerstedt G., Gustafsson K., Structural Changes in Lignin During Kraft Cooking, Part 5, Analysis of Dissolved Lignin by Oxidative Degradation, Journal of Wood Chemistry and Technology, 2007, 7(1), 65-80.

Gharehkhani S., Ghavidel N., Fatehi P., Kraft Lignin–Tannic Acid as a Green Stabilizer for Oil/Water Emulsion, ACS Sustainable Chemistry & Engineering, 2018, 7(2), 2370–79.

Ghavidel N., Fatehi P., Synergistic Effect of Lignin Incorporation into Polystyrene for Producing Sustainable Superadsorbent, RSC Advances, 2019, 9(31), 17639–52.

Ghavidel N, Fatehi P., Pickering/Non-Pickering Emulsions of tNanostructured Sulfonated Lignin Derivatives, ChemSusChem, 2020, 13(17), 4567–4578.

Ghavidel N., Sulfo-functionalization of Lignin and its Impact on the Stabilization of Colloidal Systems, PhD thesis, Lakehead University, 2021

Ghavidel N, Fatehi P., Interfacial and Emulsion Characteristics of Oil–Water Systems in the Presence of Polymeric Lignin Surfactant, Langmuir, 2021, 37(11), 3346–3358.

Ghosh, S., Rousseau D., Emulsion Breakdown in Foods and Beverages, Chemical Deterioration and Physical Instability of Food and Beverages, 2010, 260–295.

Goodarzi F, Zendehboudi S., A Comprehensive Review on Emulsions and Emulsion Stability in Chemical and Energy Industries, Canadian Journal of Chemical Engineering, 2019, 97(1), 281–309.

Graef V., Depypere F., Minnaert M., Dewettinck K., Chocolate Yield Stress as Measured by Oscillatory Rheology, Food Research International, 2011, 44(9), 2660–65.

Guion, T.H., Hood J., Viscosity Profiles of Printing Thickeners at High Shear Rates and Their Use in Predicting Paste Flow in Screen Printing, 2019, AGRIS, 55(8), 498-508.

Hasan A, Fatehi P., Cationic Kraft Lignin-Acrylamide as a Flocculant for Clay Suspensions, 1, Molecular Weight Effect, Separation and Purification Technology, 2018, 207, 213–21.

He W., Gao W., Fatehi P., Oxidation of Kraft Lignin with Hydrogen Peroxide and Its Application as a Dispersant for Kaolin Suspensions, ACS Sustainable Chemistry and Engineering, 2017, 5(11), 10597–605.

He W., Zhang Y., Fatehi P., Sulfomethylated Kraft Lignin as a Flocculant for Cationic Dye, Colloids and Surfaces, A Physicochemical and Engineering Aspects, 2016, 503, 19–27.

He W., Fatehi P., Preparation of Sulfomethylated Softwood Kraft Lignin as a Dispersant for Cement Admixture, RSC Advances, 2015, 5(58), 47031–39.

Healy R., Reed R., Stenmark D., Multiphase Microemulsion Systems, Society of Petroleum Engineers Journal, 1976, 16(03), 147–60.

Henrikki M., Smyth M,. Leskinen T., Johansson L., Osterburg M., All Lignin Approach to Prepare Cationic Colloidal Lignin Particles, Stabilization of Durable Pickering Emulsions, Green Chemistry, 2017, 19(24), 5831–40.

Heymann L., Peukert S., Aksel N., Investigation of the Solid–Liquid Transition of Highly Concentrated Suspensions in Oscillatory Amplitude Sweeps, Journal of Rheology, 2002, 46(1), 93–112.

Hopa D, Fatehi P., Using Sulfobutylated and Sulfomethylated Lignin as Dispersant for Kaolin Suspension, Polymers, 2020, 12(9), 2046.

Hu M, Russell T., Polymers with Advanced Architectures as Emulsifiers for Multi-Functional Emulsions, Materials Chemistry Frontiers, 2021, 5(3), 1205–20.

Hunkeler D., Mechanism and kinetics of the persulfate-initiated polymerization of acrylamide, 1991, 24(9), 2160–2171.

Inwood J., Pakzad L., Fatehi P., Com Production of Sulfur Containing Kraft Lignin Products, BioRes, 2018, 13(1), 53–70.

Kai D, Tan M., Chee P., Chua Y., Yap Y., Loh X., Towards Lignin-Based Functional Materials

in a Sustainable World, Green Chemistry, 2016, 18(5), 1175–1200.

Kazzaz A, Hosseinpour Z, Fatehi P., Interaction of Sulfomethylated Lignin and Aluminum Oxide, Colloid and Polymer Science, 2018, 296(11), 1867–78.

Konduri M., Kong F., Fatehi P., Production of Carboxymethylated Lignin and Its Application as a Dispersant, European Polymer Journal, 2015, 70, 371–83.

Konduri M., Fatehi P., Designing Anionic Lignin Based Dispersant for Kaolin Suspensions Colloids and Surfaces: Physicochemical and Engineering Aspects, 2018, 538, 639–50.

Kong F., Wang Sh, Gao W., Fatehi P., Novel Pathway to Produce High Molecular Weight Kraft Lignin-Acrylic Acid Polymers in Acidic Suspension Systems, RSC Advances, 2018, 8(22), 12322–36.

Laurichesse S., Avérous L., Chemical Modification of Lignins, Towards Biobased Polymers, Progress in Polymer Science, 2014, 39(7), 1266–90.

Li Sh., Willoughby J., Rojas O., Oil-in-Water Emulsions Stabilized by Carboxymethylated Lignins, Properties and Energy Prospects, ChemSusChem, 2016, 9(17), 2460–69.

Liu Ch, Wu Sh, Zhang H., Xiao R., Catalytic Oxidation of Lignin to Valuable Biomass-Based Platform Chemicals, A Review, Fuel Processing Technology, 2019, 191, 181–201.

Liu Q., Luo L., Zheng L., Lignins, Biosynthesis and Biological Functions in Plants, International Journal of Molecular Sciences, 2018, 19(2), 335.

Liu Y., Li K., Preparation and Characterization of Demethylated Lignin-Polyethylenimine Adhesives, The journal of adhesion, 2007, 82(6), 593-605.

Lugo C., Alberto C., Rojas O., Saloni D., Application of Complex Fluids in Lignocellulose Processing, Journal of Colloid and Interface Science, 2012, 381(1), 171–79.

Magual A, Horváth-Szabó G., Masliyah J., Acoustic and Electroacoustic Spectroscopy of Water-in-Diluted-Bitumen Emulsions, Langmuir, 2005, 21(19), 8649–57.

Maphosa Y., Jideani V., Factors Affecting the Stability of Emulsions Stabilised by Biopolymers, Science and Technology Behind Nanoemulsions, 2018, Doi, 10.5772, intechopen, 75308.

McLean J., Kilpatrick P., Effects of Asphaltene Solvency on Stability of Water-in-Crude-Oil Emulsions, Journal of Colloid and Interface Science, 1997, 189(2), 242–53.

Mohammed R., Bailey A., Luckham P., Taylor S., The Effect of Demulsifiers on the Interfacial Rheology and Emulsion Stability of Water-in-Crude Oil Emulsions, Colloids and Surfaces: Physicochemical and Engineering Aspects, 1994, 91, 129–39.

Mondal M., Ibrahim H., Minhaz-Ul Haque M., Effect of Grafting Methacrylate Monomers onto Jute Constituents with a Potassium Persulfate Initiator Catalyzed by Fe(II), Journal of Applied Polymer Science, 2007, 103(4), 2369–75.

Moradi M., Alvarado V., Huzurbazar S., Effect of Salinity on Water-in-Crude Oil Emulsion, Evaluation through Drop-Size Distribution Proxy, Energy and Fuels, 2010, 25(1), 260–268.

Mv G., Samec J., Lignin Valorization through Catalytic Lignocellulose Fractionation, A Fundamental Platform for the Future Biorefinery, ChemSusChem, 2016, 9(13), 1544–58.

Nakama Y., Surfactants, Cosmetic Science and Technology: Theoretical Principles and Applications, 2017, 231–44.

Pan F., Li Z., Leyshon T., Rouse D., Li R., Smith C., Campana M., Webster J., Bishop S., Narwal, R., Van D., Warwicker J., Lu J., Interfacial Adsorption of Monoclonal Antibody COE-3 at the Solid/Water Interface, ACS Applied Materials and Interfaces, 2018, 10(1), 1306–16.

Panesar S., Jacob S., Misra M., Mohanty A., Functionalization of Lignin, Fundamental Studies on Aqueous Graft Copolymerization with Vinyl Acetate, Industrial Crops and Products, 2013, 46, 191–96.

Petridis L., Schulz R., Smith J., Simulation Analysis of the Temperature Dependence of Lignin Structure and Dynamics, Journal of the American Chemical Society, 2011, 133(50), 20277–87.

Qiu H., Zhao L., Assif M., Huan X., Tang T., Li W., Zhang T., Shen T., Hou Y., SnO_2 Nanoparticles Anchored on Carbon Foam as a Freestanding Anode for High Performance Potassium-Ion Batteries, Energy and Environmental Science, 2020, 13(2), 571–78.

Raya S., Saaid I., Ahmed A., Umar A., A Critical Review of Development and Demulsification Mechanisms of Crude Oil Emulsion in the Petroleum Industry, Journal of Petroleum Exploration and Production Technology, 2020, 10(4), 1711–28.

Saake B., Ralph L., Lignin, Ullmann's Encyclopedia of Industrial Chemistry, 2007, Doi,

10,1002/14356007,a15_305,pub3.

Sabaghi S., Alipoormazandarani N., Fatehi P., Production and Application of Triblock Hydrolysis Lignin-Based Anionic Copolymers in Aqueous Systems, 2021, ACS Omega 6(9), 6393–6403.

Sabaghi S., Fatehi P., Hydrodynamic Alignment and Self-Assembly of Cationic Lignin Polymers Made of Architecturally Altered Monomers, Colloids and Surfaces A: Physicochemical and Engineering Aspects, 2021, 127437.

Saraf Vasudev P., Glasser W., Engineering Plastics from Lignin, III, Structure Property Relationships in Solution Cast Polyurethane Films, Journal of Applied Polymer Science 1984, 29(5), 1831–41.

Schramm L., Laurier N., Stasiuk, Gerrard Marangoni D., Surfactants and Their Applications, Annual Reports Section C, (Physical Chemistry), 2003, 99, 3–48.

Shulga G., Shakels V., Skudra S., Bogdanovs V., Modified Lignin as an Environmentally Friendly Surfactant, Proceedings of the International Scientific and Practical Conference, 2011, 1, 276–81.

Tadros F., Emulsion Formation, Stability, and Rheology, 2013, doi, 10,1002/9783527647941.ch1

Tambe E., Sharma M., Factors Controlling the Stability of Colloid-Stabilized Emulsions, III, Measurement of the Rheological Properties of Colloid-Laden Interfaces, Journal of Colloid and Interface Science,1995, 171(2), 456–62.

Tan C., McClements D., Application of Advanced Emulsion Technology in the Food Industry: A Review and Critical Evaluation, Foods 2021, 10(4), 812.

Tarasov D., Leitch M., Fatehi P., Lignin-Carbohydrate Complexes, Properties, Applications, Analyses, and Methods of Extraction, A Review, Biotechnology for Biofuels, 2018, 11(1), 1–28.

Tejado A., Pena C., Labidi J., Echeverria J., Mondragon I., Physico-Chemical Characterization of Lignins from Different Sources for Use in Phenol-Formaldehyde Resin Synthesis, Bioresource technology, 2007, 98(8), 1655–63.

Tolbert A., Akinosho H., Khunsupat R., Naskar A., Raguaskas A., Characterization and Analysis

of the Molecular Weight of Lignin for Biorefining Studies, Biofuels, Bioproducts and Biorefining, 2014, 8(6), 836–56.

Torres L., Iturbe R., Snowden M., Leharne S., Preparation of o/w Emulsions Stabilized by Solid Particles and Their Characterization by Oscillatory Rheology, Colloids and Surfaces A, Physicochemical and Engineering Aspects, 2007, 1–3(302), 439–48.

Urbina G., García M., Brownian Dynamics Simulation of Emulsion Stability, Langmuir, 2000, 16 (21), 7975–85.

Urbina V., An Algorithm for Emulsion Stability Simulations, Account of Flocculation, Coalescence, Surfactant Adsorption and the Process of Ostwald Ripening, International Journal of Molecular Sciences, 2009, 10(3), 761–804.

Vishtal A., Kraslawski A., Challenges in Industrial Applications of Technical Lignins, BioResources, 2011, 6(3), 3547–3568.

Walstra P., Emulsions, Fundamentals of Interface and Colloid Science, 2005, 5, 1–94.

Wang D., Yang D., Huang Ch., Huang Y., Yang D., Zhang H., Liu Q., Tang T., Gamel M., Kemppi T., Perdicakis B., Zeng H, Stabilization Mechanism and Chemical Demulsification of Water-in-Oil and Oil-in-Water Emulsions in Petroleum Industry, A Review, Fuel, 2021, 286(3), 119390.

Wang S., Kong F., Gao W., Fatehi P., Novel Process for Generating Cationic Lignin Based Flocculant, Ind Eng Chem Res, 2018, 57(19), 6595–6608.

Wang J., Chen Y., Yuan S., Sheng G., Yu H., Characterization and Performance of a Novel Lignin-Based Flocculant for the Treatment of Dye Wastewater, International Biodeterioration & Biodegradation, 2018, 133, 99–107.

Witono J., Noordergraaf I., Heeres H., Janssen LPBM., Graft Copolymerization of Acrylic Acid to Cassava Starch - Evaluation of the Influences of Process Parameters by an Experimental Design Method, Carbohydrate Polymers, 2012, 90(4), 1522–29.

Wu-Jun L., Jiang H., Yu H., Thermochemical Conversion of Lignin to Functional Materials, A Review and Future Directions, Green Chemistry, 2015, 17(11), 4888–4907.

Wu D., Honciuc A., Contrasting Mechanisms of Spontaneous Adsorption at Liquid–Liquid

Interfaces of Nanoparticles Constituted of and Grafted with PH-Responsive Polymers, Langmuir, 2018, 34(21), 6170–82.

Wu J., Ma G., Recent Studies of Pickering Emulsions: Particles Make the Difference, Small Weinheim an der Bergstrasse, Germany, 2016, 12(34), 4633–48.

Xu Ch., Arancon R., Labidi J., Luque R., Lignin Depolymerisation Strategies, Towards Valuable Chemicals and Fuels, Chemical Society Reviews, 2014, 43(22), 7485–7500.

Xu D., Bai B., Meng Z., Zhou Q., Li Z., Lu Y., Wu H., Hou J., Kang W., A Novel Ultra-Low Interfacial Tension Nanofluid for Enhanced Oil Recovery in Super-Low Permeability Reservoirs, Society of Petroleum Engineers - SPE Asia Pacific Oil and Gas Conference and Exhibition, APOGCE, 2018, 192113.

Xu H, Li Y, Zhang L., Driving Forces for Accumulation of Cellulose Nanofibrils at the Oil/Water Interface, Langmuir, the ACS journal of surfaces and colloids, 2018, 34(36), 10757–63.

Yang K., Liu Z., Wang J., Yu W., Stress Bifurcation in Large Amplitude Oscillatory Shear of Yield Stress Fluids, Journal of Rheology, 2017, 62(1), 89.

Zakzeski J, Bruijnincx P., Jongerius A., Weckhuysen B., The Catalytic Valorization of Lignin for the Production of Renewable Chemicals, Chemical Reviews, 2010, 110(6), 3552–99.

Zembyla M., Murray B., Sarkar A, Water-in-Oil Emulsions Stabilized by Surfactants, Biopolymers and/or Particles, A Review, Trends in Food Science and Technology, 2020, 104, 49–59.

Zhao X., Yu G., Li J., Feng Y., Zhang L., Peng Y., Tang Y., Wang L., Eco-Friendly Pickering Emulsion Stabilized by Silica Nanoparticles Dispersed with High-Molecular-Weight Amphiphilic Alginate Derivatives, ACS Sustainable Chemistry and Engineering, 2018, 6(3), 4105–4114.

Zhou M., Qiu X., Yang D., Lou H., Ouyang X., High-Performance Dispersant of Coal-Water Slurry Synthesized from Wheat Straw Alkali Lignin, Fuel Processing Technology, 2007, 88, 375–382.